3-2005

Lethality of *Bacillus anthracis* Spores Due to Short Duration Heating Measured Using Infrared Spectroscopy

Kristina M. Goetz

LETHALITY OF *BACILLUS ANTHRACIS* SPORES DUE TO SHORT DURATION HEATING MEASURED USING INFRARED SPECTROSCOPY

THESIS

Kristina M. Goetz, Captain, USAF
AFIT/GNE/ENP/05-04

DEPARTMENT OF THE AIR FORCE
AIR UNIVERSITY
AIR FORCE INSTITUTE OF TECHNOLOGY

Wright-Patterson Air Force Base, Ohio

The views expressed in this thesis are those of the author and do not reflect the official policy or position of the United States Air Force, Department of Defense, or the United States Government.

AFIT/GNE/ENP/05-04

LETHALITY OF *BACILLUS ANTHRACIS* SPORES DUE TO SHORT DURATION HEATING MEASURED USING INFRARED SPECTROSCOPY

THESIS

Presented to the Faculty

Department of Engineering Physics

Graduate School of Engineering and Management

Air Force Institute of Technology

Air University

Air Education and Training Command

in Partial Fulfillment of the Requirements for the

Degree of Master of Science in Nuclear Engineering

Kristina M. Goetz, BS
Captain, USAF

March 2005

AFIT/GNE/ENP/05-04

LETHALITY OF *BACILLUS ANTHRACIS* SPORES DUE TO SHORT DURATION HEATING MEASURED USING INFRARED SPECTROSCOPY

Kristina M. Goetz, BS
Captain, USAF

Approved:

Larry W. Burggraf (Chairman)	date
Charles A. Bleckmann (Member)	date
Guangming Li (Member)	date

Abstract

Anthrax has long been viewed as a potential bio-terrorist weapon. Scenarios have been developed to include counterforce strikes on enemy stockpiles of the biological agents. So called "Agent Defeat" weapons include bomb detonations which use heat to neutralize the bacteria. In this research, *Bacillus anthracis* spores were subjected to bursts of heat lasting on the order of one second in duration using a laser system to simulate the explosive environment. Heating times and temperatures were varied to establish a method to characterize the relationship between heating time, heating temperature, and spore viability. Spores were grown in culture, mechanically washed, suspended in sterilized water, and deposited on sterile glass cover slips. Heating was accomplished using a laser *in situ.* Two heating temperatures were examined at three variations of heating time ranging from 1.2 to 4.2 seconds. The higher temperature was adequate to neutralized the spore samples for both heating times. The lower temperature neutralized a portion of the spores during the shortest heating time, and sterilized the sample at the longest heating time. Before and after heating Raman spectra were obtained of the spores in order to characterize spectral differences related to neutralization by heat. Subtle spectral differences were identified with the 1013 cm^{-1} peak resulting from CaDPA in the spore wall. This change indicates a change in the integrity of the spore wall resulting from the heating. Overall, a methodology was developed to correlate heating time, temperature, and spore lethality. Further research using these methods can provide detailed time/temperature profiles for a wider variety of heating variations.

Acknowledgments

First I would like to extend my sincere thanks to my advisor, Dr. Burggraf. He took the time out of his busy schedule to patiently and thoroughly guide me whenever I needed it. Without his unwavering support and remarkable base of knowledge, this effort would not have been possible. To my other advisor, Dr. Bleckmann, I say thank you for being one of the most patient and approachable professors I have ever had. Your guidance through the microbiology of this research was crucial to its completion. I would also like to say a special thank you to Dr. Li, who spent hours in the lab trying to teach a fledgling experimentalist how to actually run a successful experiment.

I would also like to thank Dr. Eric Holwitt and the Air Force Research Laboratories Biomechamisms and Modeling Branch for their support during this research. These professionals took time out of their already busy schedules to teach me hands-on microbiology and share valuable experience with me. Special thanks goes to Dr. Kiel, LtCol Buxó, Ms. Heathman, and Ms. Franze.

Also, to Mr. Kevin Gross and Dr. Glen Perram, your support late in the game made all the difference in successfully resolving temperature measurements. For taking time out from your own work to help a student in need, I say a resounding thank you.

Another thank you goes out to the Department of Physics here at the Air Force Institute of Technology. Their guidance and material support made this effort possible.

Finally, I would like to say a most important thank you to my family and my best friend, my husband. You endured AFIT as well over the last eighteen months, and I could not have done it without you. Thank you for being so supportive and understanding during it all.

Table of Contents

Page

List of Figures

Page

List of Tables

Page

LETHALITY OF *BACILLUS ANTHRACIS* SPORES DUE TO SHORT DURATION HEATING MEASURED USING INFRARED SPECTROSCOPY

I. INTRODUCTION

Overview

Bacillus anthracis, the causative agent of anthrax, has long been considered a potential bio-terrorist weapon. In October 2001, a release of anthrax spores through the US Postal Service made that threat a reality. Since that time, five people have died from inhalational anthrax and over a dozen more sickened (Atlas, 2002: 179). It has become a scientific priority to develop faster detection methods and more effective neutralization of anthrax spores in broad public areas. Political and military emphasis has been placed on counterterrorism of this and other pathogens. Beyond the response to a public release of harmful microorganisms, focus has also been placed on destroying known stockpiles of bio-weapons before any such event occurs. Much research has gone into developing new "agent defeat" weapons responsible for targeting and destroying stores of chemical and biological (CB) weapons. Accurately predicting the neutralization of these harmful agents for defined target areas is a fundamental requirement for assessing the effectiveness of the agent defeat concept. Currently there are algorithms which predict the neutralization effect of various weapon environments (e.g. radiation, heat, combustion, chemical reactions) on a number of CB agents. There is still much to learn about agent response to a conventional explosion.

This project is primarily concerned with one of the counterterrorism scenarios described above. A series of experiments were developed to simulate using a conventional explosive device to destroy a stockpile of *Bacillus anthracis* (*B.a.*) spores. The spores were subjected to a variety of high temperatures, in keeping with an explosion (>500 ºC) over short durations of time also consistent with the explosive environment (on the order of seconds). The relationship between temperature delivered and time of heating on the survivability of the bacterial spores was examined. Analysis of spores before and after heating using Raman spectroscopy was also accomplished to study the differences in living versus dead anthrax spores which may be correlated with heating damage. Expanding the current knowledge base and experimental record will serve to aid in determining the feasibility of a conventional explosive agent defeat weapon.

Purpose of Research

The purpose of this research is to examine the lethality of high temperatures delivered over a period of tenths of seconds to seconds on *Bacillus anthracis* spores. The interest in applying the heat in such short intervals is to recreate the bomb detonation environment felt by the spores. Studies of the time-dependent spectral signature of various explosive devices have been made at the Air Force Institute of Technology (AFIT) by Orson et al. Their results suggest that the peak temperature released from a small (100-400 lb) conventional munitions explosion can reach 1578 K (Orson and others, 2003: 104). The heat from the bomb peaks immediately after detonation and continuously decreases over a period of several seconds (Orson and others, 2003: 105). Lethality measurements on *B.a.* spores have been made with long-duration heating in the

past (Fernelius and others, 1957: 300; Spotts-Whitney and others, 2003: 623). The timeframes studied, however, typically only go down to about one minute of heating. At these relatively long times, it is unnecessary to heat the spores to temperatures near the 1500 K generated by an HE explosion in order to neutralize them. It is clear from past research, however, that the shorter time over which the heat is applied to the spores, the higher the temperatures necessary to neutralize them. The novelty of this research is the extremely short timeframe that was examined (tenths of seconds to seconds) and the high temperatures employed (> 500 ºC).

In this work, heated spores were resuspended in culture in order to measure lethality; however, Raman spectroscopy is a potential alternative to characterize thermal neutralization of the spores. Although Raman spectroscopy has often been used to study *Bacillus* organisms in the past, no spectral comparisons of live versus dead bacteria were found. Since this relationship has not been well characterized in the past, it was not clear prior to this work, what the Raman microscope would reveal. The precise bio-chemical changes which occur in a dry heated spore and lead to its death are not absolutely clear. It is known that hydrolysis reactions take place within the DNA of the heated cell, causing damage. These heat-induced chemical changes lead to the spore's ultimate destruction, and may be detectable using the Raman spectrometer.

The goal of this research is to quantify the time and temperature conditions necessary to ensure death of the *Bacillus anthracis* spores. Spore death was defined as those spores which were longer able to be germinated by conventional microbiological cultures. This assumed that the bacteria were no longer metabolically active. A sample

was considered “sterilized” if no germination was present after it was transferred to culture and given the opportunity to germinate.

Bacillus anthracis was chosen because it is the pathogenic cause of anthrax (Willet, 1992a, 615) and a known WMD terrorist threat. It also represents the most challenging agent defeat mission. Time/temperature profiles that defeat these spores are adequate to destroy most chemical and other biological weapons. Several species of *Bacillus* are very closely related genetically. It is reasonable to assume that what kills the *anthracis* strain could also kill other similar strains. All research was conducted using only the *B.a.* Sterne strain on the basis of its availability and its importance as a biological agent simulant.

Research Objectives

The ultimate goal of this research was to develop and demonstrate a method to relate heating time, temperature, and lethality measurements on *Bacillus anthracis* spores. This would be accomplished through the following minor goals: (1) devise an experimental methodology that would permit the controlled heating of bacterial spores; (2) characterize the response of viable *Bacillus anthracis* spores using Raman spectroscopy; (3) apply the developed heating procedure using a laser to deliver a short burst of heat to each spore sample of *Bacillus anthracis*; (4) characterize the spores for a second time using the Raman spectrometer and compare the spectral characteristics in search of distinctive differences that would differentiate viable and nonviable biological material; and (5) attempt to grow-up the spores in culture to confirm which samples contain viable bacteria versus dead bacteria.

Scope of Research

This research was limited in scope in several areas. First, only *B.a.* was studied. This decision was made because of the availability of the spore stock, its applications to bio-terrorism, and the presumption that other, related strains would exhibit similar responses to the heating.

Second, although *B.a.* can exist in vegetative cell form as well as spore form, only cells which had fully sporulated were studied. The spores are very hardy organisms and can withstand significantly more harsh environments than the vegetative cells (Liu and others, 2004:164). The viability of the most survivable form of the organism was examined. Also, it is believed that the spore form of *B.a.* is singularly responsible for the inhalational anthrax infection (Liu and others, 2004:164), which makes them important for bio-terrorism.

Third, only one laser wavelength was used to collect the Raman spectra, 785 nm. Although prior research has shown that shorter wavelengths are more optimized for viewing the spores (Esposito and others, 2003: Ghiamati and others, 1992), equipment constraints dictated that the 785 nm laser would be the most suitable option for this research. The 785nm wavelength laser is advantageous for samples that photoluminesce. The spores demonstrate little photoluminescence, however, so this advantage is nullified. This longer wavelength laser still allowed the collection of spore spectra, but perhaps not as intense as would have been possible with a laser in the visible or UV regions of the spectrum where the Raman scattering efficiency by the spores is thought to be larger.

Finally, only a small number of samples were studied for each heating time and temperature combination. Ideally, many more samples of each pairing would have been

studied. The time required for spectral collection and bacterial growth, however, limited the sample size to what is included here.

II. Literature Review

Overview

This research sought to link applied heat to *Bacillus anthracis* spore viability and relate that viability to quantifiable features of Raman spectra from the spores. Multiple scientific disciplines were included to make this research possible. This chapter is divided into five main sections. The first describes the microorganisms, including why they were chosen, bacterial characteristics, sporulation and germination. The second part summarizes information from prior research on heat inactivation of spores, and discusses cellular processes that cause spore death from heating. The third part concentrates on the bomb detonation agent defeat concept, including spectral radiance from the explosions, peak temperatures, and heating times. Fourth, Raman spectroscopy will be reviewed, including theory, spectrometer configuration, and suitability for biological applications. The fifth section briefly describes infrared spectroscopy, including theory, spectrometer configuration and considerations when measuring temperature delivered to the spores by the laser.

The Genus *Bacillus*

The defining characteristic of the *Bacillus* genus is the production of resistant endospores in the presence of oxygen (Logan and Turnbull, 2003: 445). *Bacillus* members are generally gram-positive, rod-shaped, aerobic or facultative anaerobic organisms (Logan and Turnbull, 2003: 445). They can be found in many natural environments, including all kinds of soil (hot or cold, alkaline or acidic, fertile or desert)

and bottom deposits of marine or freshwater bodies (Logan and Turnbull, 2003: 445). Many species can also act as obligate pathogens of animals.

Description of Bacillus anthracis. Bacillus anthracis, the etiological agent of anthrax, is the only major pathogen in the genus Bacillus. Anthrax was first isolated by Robert Koch in 1877 (Willet, 1992a: 633). Using anthrax, the principle of live bacterial vaccination was first successfully tested by Louis Pasteur in 1881 (Mock and Fouet, 2001: 661). The disease is primarily found in herbivores, but can be carried by any mammal.

The bacteria are gram-positive, rod-shaped, aerobic, facultative anaerobic, nonmotile, and endospore-forming (Mock and Fouet, 2001: 648). The vegetative form of the bacteria is square-ended and capsulated. The rods are 5 to 10 microns in length and 1 to 3 microns in diameter (Willet 1992a: 633). When these vegetative cells begin to sporulate, they carry centrally located, ellipsoidal spores. A stained sample of *B.a.* is shown below in Figure 1. The endospores are beginning to form and are visible within some vegetative cells.

Typical *Bacillus* colonies are 2 to 7 mm in diameter, with *B.a.* generally staying in the range of 2 to 3 mm (Logan and Turnbull, 2003: 454). These *B.a.* colonies are nonhemolytic on blood agar, and can show spiking and comma-shaped tailing along inoculation streaks (Logan and Turnbull, 2003: 454). Colonies are raised and grayish-white, with irregular edges (Willet, 1992a: 633).

There are three antigens of *B.a.* including (1) a capsular polypeptide, (2) a protein toxin, and (3) a polysaccharide somatic antigen. The third antigen is a component of the

cell wall, while the first two are necessary for disease (Willet, 1992a: 634). The capsule is exclusively made up of D-glutamic acid, and interferes with phagocytosis in the host mammal (Willet, 1992a: 634). The toxin consists of three components including a protective antigen (PA), a lethal factor (LF), and an edema factor (EF) (Willet, 1992a: 634). These components only achieve maximum toxicity when they are all present within the host and acting synergistically (Willet, 1992a: 635). Separately none of them is toxic. Injection of PA and LF only will still provoke death in the mammal, while combining PA and EF only will produce skin edema. PA is the necessary link able to interact with the two different enzymes (Mock and Fouet, 2001: 654).

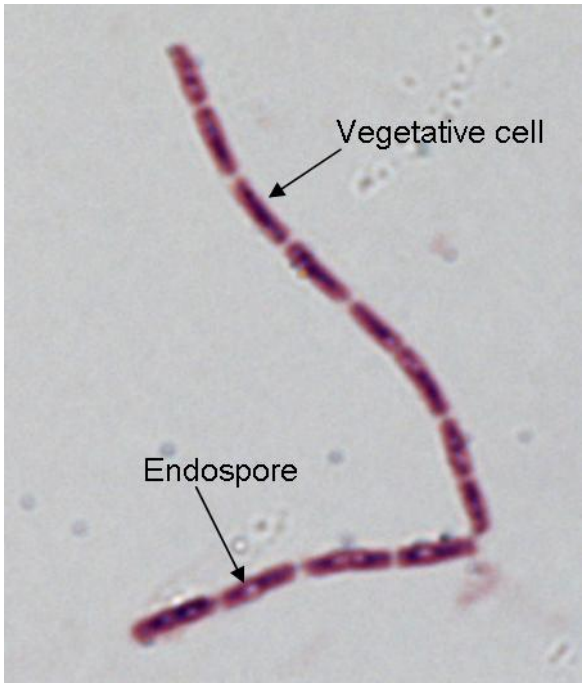

Figure 1. Gram-stained *Bacillus anthracis* vegetative cells and visible endospores

The *Bacillus anthracis* Spore

A spore represents a dormant state of the bacteria. It is extremely resistant to environmental factors such as temperature, ultraviolet (UV) radiation, pressure, and some chemical agents because of a distinct lack of metabolic activity. The spore is poised and ready to reestablish vegetative growth once conditions again become favorable. Although spores show little signs of life in their dormant stage, they possess "an alert sensory mechanism which is able to respond to specific germinants within minutes" when circumstances present themselves allowing for germination (Leuschner and Lillford, 2001: 36). Environmental conditions can affect the size, flexibility, and chemical composition of the spore. Therefore its structure is somewhat subject to variation and should not be considered absolutely fixed.

Bacillus anthracis Spore Structure. The spore is composed of several protective structures arranged in a series of concentric shells, all contributing in some way to increased durability. Two key functions of spore structure include locking the DNA into a crystalline, desiccated, and stable state, while also using an armored external shell to prevent the entrance of toxic molecules (Driks 2003: 3007). Figure 2 shows the layered structure of the spore. Each layer will be briefly described in terms of structure and basic function.

The outermost layer of the *B.a.* spore is the exosporium. Little is known about the exosporium. It is believed that since other *Bacillus* species which lack the exosporium (e.g. *Bacillus subtilis*) are still resistant to environmental stresses, that it does not serve as a protective layer, but rather plays a role in niche accommodation (Driks, 2003: 3007). The major components of the exposporium are protein, lipid, and carbohydrate (Mock

and Fouet, 2001: 651). The surface can be covered with filamentous appendages called pili which are thought to aid in spore attachment to surfaces (Mock and Fouet, 2001: 651).

Beneath the exosporium lies the spore coat (Driks, 2003: 3007). This coat is composed of two distinct layers: the thickly layered outer coat, and the finely banded inner coat. The coat composition has been shown to include over 25 proteins (Driks, 2003: 3008). Functionally the coat serves at a barrier against large toxic molecules. Recently it has also been shown that proteins exist in the coat which play a role in germination (Bagyan and Setlow, 2002: 1219). Data suggests that spore coat flexibility can vary widely among various species.

Beyond the spore coat is the forespore membrane (Driks and Setlow, 2000: 193). Little information is known about this membrane and its function. Beneath this membrane lies the cortex, which forms a tight belt around the DNA in the core in order to keep it dry (Driks, 2003: 3007). The structure of the cortex can be likened to a tightly woven fabric. This fabric allows small molecules, like water, to pass through. The core remains dry, however, because of the constricting action of the cortex (Driks, 2003: 3007). This desiccation contributes to heat resistance and dormancy of the spore. The cross linking of the woven peptidoglycan strands allows the cortex to loosen and tighten in response to ionic and pH changes sensed by the spore (Driks, 2003: 3007). A thin layer of this peptidoglycan is called the germ cell wall, and will become the initial vegetative cell wall once germination occurs (Popham and others, 1996: 15405). The remaining barrier to the core is the inner forespore membrane, about which little is known.

The spore core holds all the genetic material of the cell, including the nucleoid, enzymes, and ribosomes (Driks and Setlow, 2000: 193). The DNA is housed with several small acid-soluble proteins which serve to protect the DNA from stresses such as heat and UV radiation (Driks, 2003: 3007).

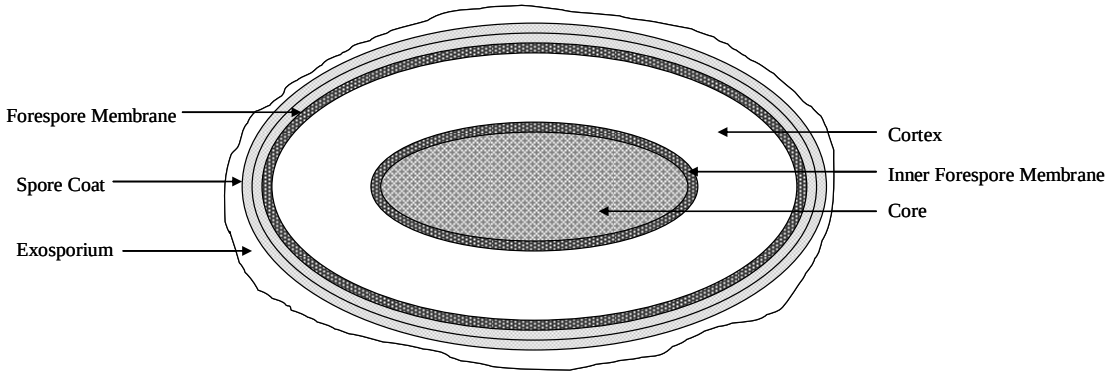

Figure 2. Structure of a *Bacillus* Spore

Sporulation. Bacillus anthracis will sporulate in soil, culture, or in the remains of dead animals (Willet, 1992a: 633). The Bacillus bacteria begin to form spores as a response to nutrient deprivation, including the depletion of either a nitrogen or carbon source (Setlow and Johnson, 2001: 34). The process of sporulation can be divided into eight stages, which may take place in as little as eight hours (Setlow and Johnson, 2001: 35). Initially the term "endospore" is used because the spores form inside the vegetative cell (Setlow and Johnson, 2001: 35). The eight stage process is outlined in Figure 3 (Setlow and Johnson, 2001: 35; and Driks and Setlow, 2000: 191-210).

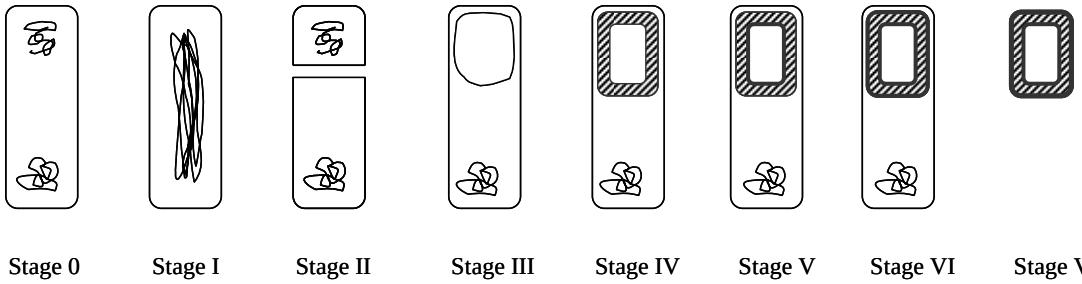

Figure 3. Stages of Sporulation

The sporulation process begins with Stage 0, the vegetative cell. Chromosome replication occurs, resulting in two distinct, yet identical nucleoids (Setlow and Johnson, 2001: 36). Stage I is not universally considered unique to the sporulation process, so it is not included in some references. For those that do include it, Stage I describes the development of an axial filament from the two nucleoids.

Stage II is referred to as "septation". It initiates the development of the forespore with the formation of a double membrane septum (Setlow and Johnson, 2001: 36). This septum divides the cell into a mother cell and the new forespore, each containing one of the two nucleoids. This division is asymmetrical, with the forespore being the smaller of the two halves. The outer of the two membranes will ultimately become the forespore membrane, while the inner will become the inner forespore membrane in the fully formed spore (Setlow and Johnson, 2001: 36). The nucleoid inside the new forespore condenses on its way to becoming the spore core.

At Stage III the cell is committed to sporulation. This is when the mother cell engulfs the forespore and the prespore protoplast is formed (Setlow and Johnson, 2001: 36). The inner and outer membranes fully surround the forespore at this point.

Stage IV is referred to as “cortex formation”. The cortex is formed when peptidoglycan is deposited between the double membranes (Setlow and Johnson, 2001: 36). The space between the membranes will become the fully formed cortex. The germ cell wall forms between the cortex and the inner forespore membrane. It is during this stage the dehydration within the spore begins (Setlow and Johnson, 2001: 36). The spore already has increased resistance to UV light and some chemicals at this point in its development (Setlow and Johnson, 2001: 36).

During Stage V (coat formation), an inner spore coat protein is deposited on the surface of the outer forespore membrane (Setlow and Johnson, 2001: 36). Dehydration of the forespore continues. During Stage VI the spore matures by depositing another outer spore coat on the surface of the inner spore coat (Setlow and Johnson, 2001: 37). This increases the spore’s resistance to environmental stresses such as heat and more harmful chemicals. It is by this stage of development that the spore has accumulated the dipicolinic acid in the spore core which is synthesized by the mother cell (pyridine-2,6-dicarboxylic acid or DPA) (Setlow and Johnson, 2001: 37). This chemical acts to protect the spore DNA from extreme environmental stresses. The spore core reaches its final level of dehydration signaling a change in permeability of the membranes (Setlow and Johnson, 2001: 37). This change is the reason for the spore’s ultimate resistance to typical bacteriological staining techniques. The spore now becomes metabolically dormant. Stage VII is referred to as “release” as the mother cell lyses and releases the mature spore into the environment (Setlow and Johnson, 2001: 37).

Germination. Germination occurs when a dormant, resistant spore senses changes in the surrounding environment and responds by becoming a metabolically

active vegetative cell (Willet, 1992b: 72). Spore germination has three stages including activation, germination, and outgrowth (Willet, 1992b: 72). The first step, activation, is reversible by the spore if conditions once again become unfavorable. Activation is triggered by heat or the presence of certain chemicals (Willet, 1992b: 72). The second step, germination, is non-reversible. For germination to occur, the spore must come into contact with many types of nutrients as well as several non-nutrient stimulants (Willet, 1992b: 72). The third and final stage of germination is outgrowth. During this time the spore synthesizes the proteins and structural components necessary to become a vegetative cell (Willet, 1992b: 72). Once the spore completes germination and returns to vegetative cell form, its increased heat resistance and hardiness are gone. It is once again a vulnerable cell.

Spore Damage Mechanisms Caused by Dry Heat

Spores are naturally resistant to many environmental stresses, including heat. However, when the temperature is raised high enough or the spore heated for a long enough time, damage will be done to these hardy cells. What follows is a brief description of damage mechanisms caused by dry heating of spores.

The spore dry heat damage mechanism largely involves hydrolysis-type of DNA in the core at the center of the spore. There are several types of hydrolysis reactions including depurination and deamination. Deamination is the removal of the amino group from one of the DNA bases. This can change the base-pairing properties of the affected base. For example, the removal of the amino group from a cytosine base may give rise to

a uracil or thymine base instead. This mutated base will then be inclined to pair with adenine, rather than the correct guanine base, changing the DNA code.

The most likely hydrolysis reaction, however, is depurination of the DNA. Depurination is harmful because it leads to a high frequency of mutations and increased numbers of single-strand breaks. N-glycosidic bonds between a purine base and its deoxyribose chain are most susceptible to this hydrolysis reaction. Depurination occurs spontaneously, and is accelerated at high temperatures. When the depurination takes place, a purine base pair (either adenine or guanine) is severed from the deoxyribose chain, as shown in Figure 4. The chain backbone is left intact, however. With this base pair missing from the chain, the DNA strand can no longer match up with the other half of its double helix. The strand is in effect "broken" because of the hydrolysis reaction. The higher the temperature applied to the spore, the greater the probability of depurination.

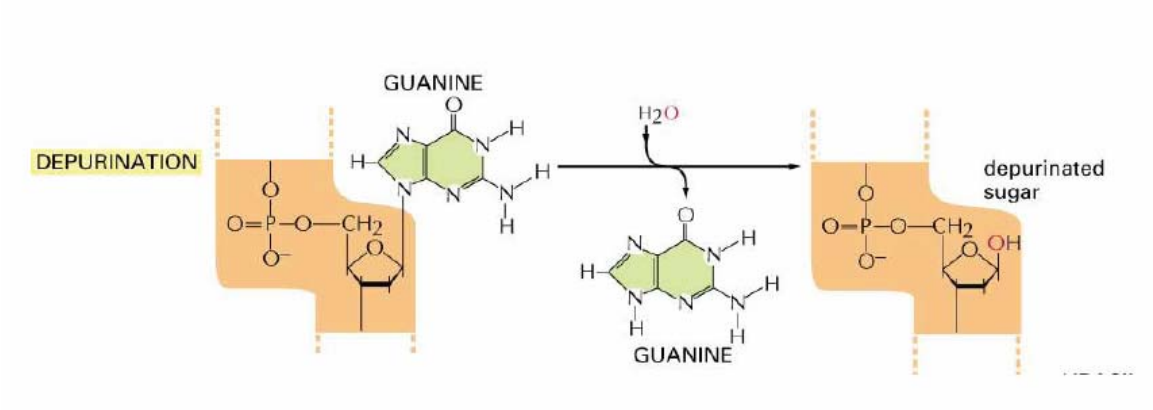

Figure 4. Depurination by Hydrolysis in Cellular DNA

The spores have some natural defense systems against this depurination threat. Alpha and beta type small acid soluble proteins (SASP) in the spore provide significant

protection to spore DNA against the damaging effects of dry heat. The role of these proteins is to bind tightly to the DNA and guard against dry heat-induced depurination. If temperatures are too high, or heat continues for a long duration of time, however, the SASP can only do so much to protect the DNA. Eventually, damage will occur within the cell, and may lead to spore death.

This idea that hydrolysis reaction rate increases with increasing temperature leads to the idea that thermal inactivation of spores might be governed by an Arrhenius relationship. It is assumed that there is a threshold damage model for heat activated cell death. If damage accumulates above this threshold, the spore will most likely die. The Arrhenius rate constant is shown below in Equation 1.

$$k = A*\exp(-E_a / RT) \quad (1)$$

where k is the first order rate constant, A is the Arrhenius pre-exponential factor (which has very weak temperature dependence), E_a is the activation energy ($Jmol^{-1}$), R is the gas constant (8.314 $Jmol^{-1}$), and T is the absolute temperature (°K).

In the case of this research, the reaction rate is not specifically of interest, but rather the threshold damage required for kill at a given heating time and constant temperature. The rate constant is integrated over heating time and related to the threshold damage, τ_p, as shown below in Equation 2.

$$\tau_p = k*t = A*t*\exp(-E_a / RT) \quad (2)$$

Therefore, we expect a plot of log heating time versus inverse heating temperature to be linear with a slope of E_a / R. One such plot will be shown in the next section in the discussion of current models of *Bacillus* heat inactivation.

The Arrhenius relationship must be further modified to take into account the chemical kinetics of the reaction. The water activity of the spore must be taken into account (represented as $\{H_2O\}^n$), since it is intimately related to the thermal reactions within the cell. It can be assumed in the case of the spores that A is independent of temperature and constant, and $\{H_2O\}$ is constant during heating, so the condition of the spore does not change during heating. Therefore, this equation can be assumed to be zero order.

Thermal Conductivity Influence on Spore Lethality Due to Heating.

Extrapolations down to very short heating times may indicate inaccurate values for heating temperature. It is believed that thermal diffusion through the spore becomes important at these very short times, and may limit damage accumulation. It can no longer be assumed at very short heating times that the spore instantaneously achieves that target heating temperature. It is useful to perform a brief calculation of the thermal diffusion characteristic time of the spore. If the heating times used during this research are long compared to this characteristic time, it can be assumed that the spores reach temperature instantaneously, and the Arrhenius relationship holds for this research.

Newton's Law of Heating applied to very short heating times is as follows:

$$\Delta t = \frac{m * C_p * \Delta x}{k * A} \tag{3}$$

where Δt is the characteristic diffusion time, k is the thermal conductivity, A is the contact area of the spore to the heat source (assumed to be $4\pi r^2$ where r is the radius of the spore, or $1x10^{-12}$ m^2), m is the spore mass, C_p is the specific heat, and Δx is the characteristic diffusion length (assumed to be spore diameter or 1μm in this case). It is also assumed that there is no temperature dependence for Δt for this calculation.

This equation can be simplified by taking into account the thermal diffusion coefficient for water at 25°C ($D_T = 1.4x10^{-7}$ m^2s^{-1}). The characteristic diffusion time then becomes:

$$\Delta t = \left(\frac{8}{3}\right)\frac{r^2}{D_T} = 1.8x10^{-6}\ \text{sec} \qquad (4)$$

Therefore, for micron-scale diffusion through a spore, the characteristic thermal diffusion time is on the order of microseconds. Since heating during this research was accomplished on the order of one second, it is not necessary to take this thermal diffusion process into account in terms of spore inactivation. The rate-limiting process damaging spores can be assumed to be the thermally activated chemical reactions. The Arrhenius relationship can, therefore, be assumed to hold for the heat inactivation.

Models for Dry Heat Inactivation

Much research has been done in the way of examining heat stress on the viability of *Bacillus* spores. The data, with very few exceptions, is comprised almost entirely of long-duration heating (greater than one minute). The focus of this research is timeframes at least an order of magnitude less than this (on the order of one second). What follows in this section is a short description of published research describing the effects of heating

on various species of *Bacillus*. Data from this research is valuable from the standpoint of trend analysis. Extrapolated temperatures necessary for rendering spores non-viable with short duration heating can be examined by reviewing this data.

Spotts-Whitney et al provided a survey of current literature which dealt with the inactivation of *Bacillus anthracis* spores after the October 2001 releases through the postal service. The portion of the survey which dealt with spore heating is included below in Table 1 (Spotts-Whitney and others, 2003: 624). Both wet heat and dry heat applied to the spores are considered in the study. It is a well-established fact in microbiology that wet heat kills microorganisms more effectively than dry heat. This is the principle behind adding water to an autoclave during sterilization. This study shows a quantization of that fact when comparing wet heating data to dry heating data. Lower temperatures and shorter heating times are required to inactivate a larger number of bacteria when wet heat is used over dry heat (Spotts-Whitney and others, 2003: 624). The data concerned with dry heat inactivation is most closely related to the experimental setup in this research. The shortest timeframe considered was 30 seconds of heating. Temperatures required for sample neutralization were at least 200ºC. If the data are plotted, as shown in Figure 5, the inactivation temperatures have a reasonably linear fit when heating time is on a logarithmic scale. Extrapolation of this data down to a heating time of one second indicates that the temperature required to inactivate the spores on would be approximately 240ºC.

Table 1. Heat Inactivation of *Bacillus anthracis* Spores from Spotts-Whitney et al

Temperature	Time	Inoculum Size	Inactivation Effect
Boiling			
100ºC	10 min	$3x10^6$	Sample Sterilized
	5 min	$7.5x10^8$	Sample Sterilized
Moist Heat			
90ºC	20 min	$1.2x10^6$	Sample Sterilized
90ºC to 91ºC	60 min	$3x10^8$	Spores Detected
100ºC	10 min	$1.2x10^6$	Sample Sterilized
100ºC to 101ºC	17 min	$1x10^5$	Sample Sterilized
105ºC	10 min	$3x10^6$	Sample Sterilized
120ºC	15 min	$2.4x10^8$	Sample Sterilized
Dry Heat			
140ºC	>90 min	$6x10^3$ to $1.2x10^4$	Sample Sterilized
150ºC	10 min	$6x10^3$ to $1.2x10^4$	Sample Sterilized
160ºC	10 min	$6x10^3$ to $1.2x10^4$	Sample Sterilized
180ºC	2 min	$6x10^3$ to $1.2x10^4$	Sample Sterilized
190ºC	1 min	$6x10^3$ to $1.2x10^4$	Sample Sterilized
200ºC	30 sec	$6x10^3$ to $1.2x10^4$	Sample Sterilized

Fernelius et al made many measurements of *Bacillus anthracis* survivability in 1958. Experimental data from these *B.a.* heat inactivation studies were used to develop a predictive model of lethality behavior. Calculated points from their predictive model are displayed in Figure 5 (Fernelius et al, 1958: 302). They began with experimental data for several heating times and temperatures. They developed a mathematical relationship based on initial and final spore concentrations, a death rate constant, and the measured inactivation times (Fernelius et al, 1958: 301). This model was also based on the Arrhenius relationship described in the previous section. This relationship allowed them to extrapolate and interpolate to whatever heating times and temperatures they desired.

Their results indicate a temperature of approximately 120ºC to inactivate the spores in one second. This is significantly lower than the 240ºC indicated by Spotts Whitney et al.

Finally, data from experiments by Molin and Östlund appears in Figure 5 (Molin and Östlund, 1976: 557). They have an actual data point at 1 second heating time which corresponds to 190ºC. All of their measurements were done using *Bacillus subtilis*, (*B.s.*) but as discussed earlier, each species of *Bacillus* spores should exhibit very similar resistance to heating, so it is assumed that their results would be comparable to work done using *B.a.*

Figure 6 shows the Arrhenius-style plot of the same data displayed in Figure 5. This Arrhenius relationship was described in the previous section on spore damage mechanisms caused by dry heat. A linear relationship between log heating time and inverse heating temperature is shown, supporting the idea of a thermally activated Arrhenius rate reaction within the spores. It cannot be assumed, however, that this relationship will hold for ever-decreasing heating times. At some very hot temperature and very short heating time, it is likely that the time for thermal transport through the spore wall to the DNA will become important. For heating times on the order of a few seconds, however, it is assumed that the Arrhenius relationship holds, as demonstrated in the previous section with the characteristic diffusion time calculation.

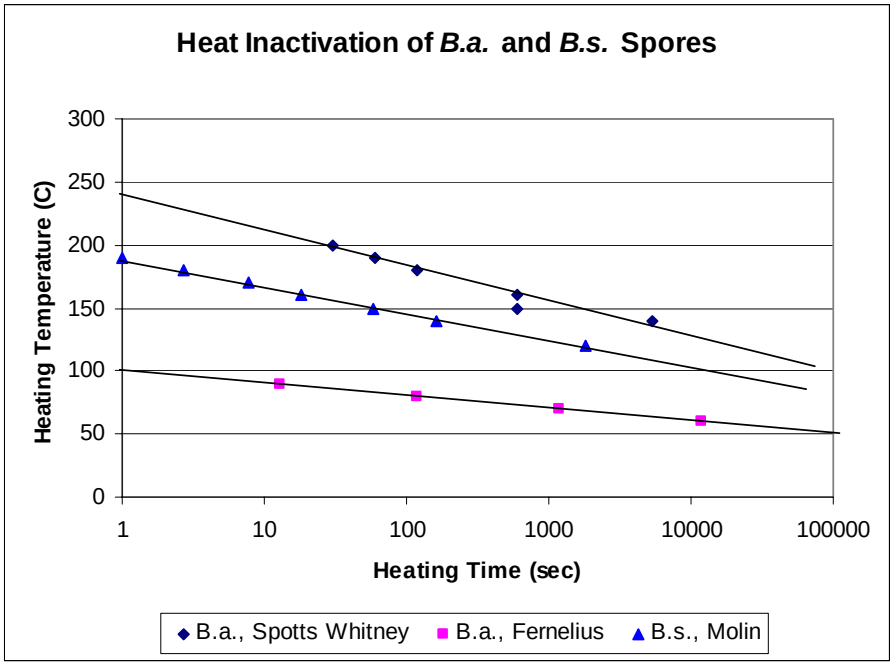

Figure 5. Plot of Dry Heat Inactivation Data for *B.a.* and *B.s.* from Three Sources Diamonds represent dry heat inactivation data for *B.a.* shown in Table 1 from Spotts Whitney et al. Squares are 99% inactivation data for *B.a.* from model developed by Fernelius et al. Triangles are dry heat inactivation data for *B.s.* from Molin and Östlund.

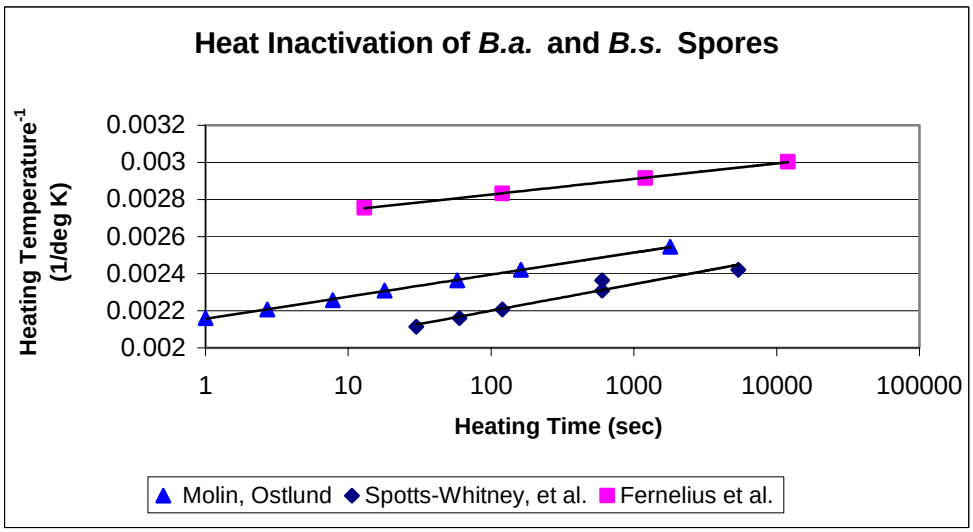

Figure 6. Plot of Dry Heat Inactivation Data Plotted in Arrhenius Style Same three sources listed in Figure 5.

This data indicates that the temperature required to inactivate a given sample of *Bacillus* spores in a very short time interval will lie within a range. Estimates were as low as 120ºC and as high as 240 ºC in the three papers covered here. These variations may be partially attributed to varied sporulation conditions of the *Bacillus* organisms. Heat resistance of spores can be greatly affected by environmental conditions during the sporulation process. Temperature, humidity, and time spent at each sporulation stage can influence a spore's ability to withstand heat (Faille et al, 2002: 1930-6). Sporulating cells of *Bacillus* which are subjected to mild heat shock treatment develop spores which exhibit increased heat resistance compared to spores grown from untreated cells (Faille et al, 2002: 1930). Since none of the papers looked at here have actual data points in the fraction of a second heating range, the focus of this work is to devise a method to characterize dry heat inactivation in one second or less. Spore heat resistance will still be comparable to only those other spores grown under identical conditions, however with the method in place, studies can be made of any growth conditions desired.

Agent Defeat Weapons

Weapons developed to neutralize biological and chemical agents are termed "agent defeat" weapons. Those developed for use against biological agents can employ heat, chemicals, UV radiation, and other techniques to destroy the microorganisms. What follows is a short discussion of weapon concepts which utilize heat as the inactivation method as well as a brief description of research conducted on bomb detonation fireballs demonstrating heating times and temperatures.

Very little information is available in the open literature concerning the times and temperatures produced by agent defeat weapons that use heat as an inactivation method. The information that is available is very general. Searches for temporal and spectral information related to bomb detonations of any sort, not just exclusive to agent defeat, come up with very little as well. Reports say things like explosions generate temperatures which are "very hot" or which burn for "long times." The specifics of heating times and temperatures associated with the types of explosives which are of interest here are mostly unavailable in the open literature. Consequently, what follows is a short review of data that was found to contain some specific information on the duration and extent of heating of conventional explosions.

One proposed agent defeat warhead is the HTI-J-1000 (globalsecurity, 2002). This high temperature incendiary J-1000 Kinetic Energy Penetrator Warhead can be used to destroy biological or chemical manufacturing and storage facilities (globalsecurity, 2002). This a two stage device would neutralize microorganisms with a combination of heat from the incendiary along with a second stage chemical component release (monatomic chlorine and fluorine gases, hydrochloric and hydrofluoric acid) (globalsecurity, 2002). The munition to be used in the warhead is 300 lb of pelletised titanium boron lithium perchlorate intermetallic high-temperature fill (globalsecurity, 2002). This filling can burn at temperatures of 1000ºF (537ºC) for a "long time" (globalsecurity, 2002). This period of time is not specifically identified by the source, but it is assumed that it is a period of at least a few seconds based on the information provided from Orson et al which follows. The warhead is designed to explode with low overpressure so as to prevent remnants of the biological stockpile to be ejected from the

facility. The chlorine and fluorine compounds are left as by-products of the high-temperature incendiary reaction (globalsecurity, 2002).

In the AFIT/ENP group headed by Dr. Perram, research is ongoing to characterize time-temperature profiles and spectra of high explosive (HE) fireballs using very similar spectroscopy to what was used in this work (Orson and others, 2003: 101). Four different bomb sizes were studied ranging from <100 lbs to >600 lbs of explosives (Orson and others, 2003: 102). The types of explosives used included RDX, TNT, and H-6 (Orson and others, 2003: 102). Results of these experiments indicate that heating from all bombs studied lasts for approximately 4 seconds, with peak temperatures being reached in under 0.5 seconds (Orson and others, 2003: 104-5). The peak temperature measured from a small RDX bomb (< 100 lbs) using an HgCdTe detector was found by fitting a Plackian function to the collected infrared spectrum. Corrections for atmospheric transmission and background were taken into account with the Planckian fits. The distribution indicated a peak temperature of 1578 K (Orson and others, 2003: 104). Similar measurements of large H-6 bombs (> 600 lbs) indicated peak temperatures of approximately 1600 K (Orson and others, 2003: 105).

These measurements can serve as a good basis for estimates of heating times and temperatures generated by agent defeat weapons. For the purposes of this research, it was assumed that heating times of 0-4 seconds and peak temperatures of ~1600 K would be necessary to simulate the explosive environment created by a nominal agent defeat warhead.

Raman Spectroscopy

One of the tools used in this work to study the *Bacillus anthracis* spores was Raman spectroscopy. In 1928 an Indian physicist named Chandrasekhra Venkata Raman discovered that in some cases of radiation scattering, a small fraction of the scattered radiation differs in wavelength from the incident radiation (Ferraro and Nakamoto, 1994: 1). It was realized that these differences were the result of the chemical structure of the molecules being bombarded with the radiation. He was awarded the Nobel Prize in physics in 1931 for his discovery and subsequent exploration of this phenomenon (Skoog and others, 1997: 429).

Since the discovery of Raman scattering, many advances have been made in the applications of the technology. With the widespread availability of lasers in the 1960s, spectra became much easier to obtain. The advent specifically of near-infrared laser sources has decreased the problem of fluorescence in the sample which had previously deterred many scientists from using Raman spectroscopy (Skoog and others, 1997: 429). As new technologies evolve, Raman spectroscopy finds more applications across a wide array of sciences. General information about the theory of Raman spectroscopy will be discussed, along with biological applications related to this research.

Overview of Raman Spectroscopy. Raman spectra are obtained by irradiating a chosen sample with monochromatic radiation in the near-infrared or visible spectrum (Skoog and others, 1997: 430). When light is scattered off of a molecule, most of the photons are elastically scattered (scattered photons which have the same energy as the incident photons). A small fraction (approximately 1 in 10^5 photons) undergoes inelastic scattering, typically to frequencies lower than the incident photon frequency (Ferraro and

Nakamoto, 1994: 15). When this type of scattering occurs, the process is known as the Raman effect. The intensity of the Raman lines created by this scattering is at most 0.001% of the intensity of the radiation source (Skoog and others, 1997: 430). Collection efficiency is, therefore, very important to successful Raman spectroscopy.

The Raman effect can occur with a change in vibrational, rotational, or electronic energy of the molecule (Ferraro and Nakamoto, 1994: 15). The difference between the energies of the incident and Raman scattered photon is equal to a ro-vibrational energy of the molecule. The spectra generated by Raman spectroscopy during this research plot the intensity of scattered photons versus vibrational energy difference from the incident radiation. The Raman effect arises specifically when an incident photon interacts with the electric dipole of a molecule (Skoog and others, 1997: 432). At room temperatures the thermal population of vibrational excited states is low. Therefore, the initial vibrational state is most likely the ground state and the scattered photon will have lower energy than the incident photon as shown in Figure 7a (Ferraro and Nakamoto, 1994: 16). This is called Raman Stokes scattering. A small fraction of the molecules are also in excited vibrational states. Raman scattering from these states leaves the molecule in the ground state. The scattered photon therefore appears at a higher energy than the incident photon (Ferraro and Nakamoto, 1994: 16). This is called Raman anti-Stokes scattering and is shown in Figure 7b.

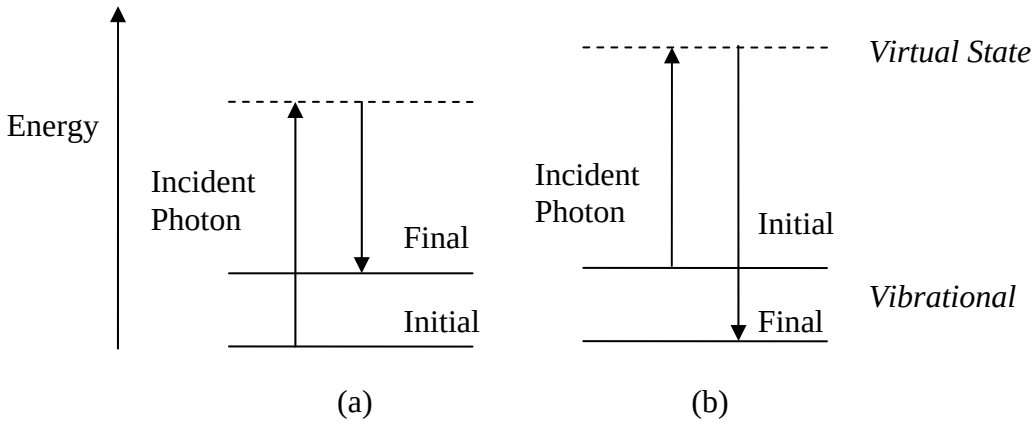

Figure 7. Energy level diagram for Raman scattering
(a) Stokes scattering, (b) Anti-Stokes scattering

The anti-Stokes spectrum is generally weaker than the Stokes spectrum. For this reason, many studies which use Raman spectroscopy only take into account the Stokes side of the spectrum. The ratio of anti-Stokes to Stokes intensities at any given vibrational frequency can be used as a measure of temperature (Ferraro and Nakamoto, 1994: 12). The ratio of the anti-Stokes to Stokes lines will always increase with temperature because more molecules will be in an initially excited vibrational state. This form of temperature measurement has good accuracy, but was not used during this research because of equipment collection efficiency issues.

The intensity of a Raman signal is proportional to the number of molecules in the sample which lead to scattered light of that wavelength. The locations of the vibrational energy peaks in a Raman signal can be used to identify materials in a sample. In this case, information regarding the molecular constituents of a *B.a.* spore can be gained. If the spore changed structure as a result of lethal heating, it is reasonable to assume that changes in the molecules of the spore occurred on a vibrational level. Differences in the

Raman spectrum of the spore may be detectable. Examination of this phenomenon is the impetus for the use of Raman spectroscopy in this research.

Description of the Raman Spectrometer. A schematic of the Raman spectrometer setup used during this research is shown in Figure 8 (Kaiser, 2001a: 7-4). A short description of the main components follows the diagram. The configuration of the spectrometer was never changed during this work, and all spectra were collected using this identical setup.

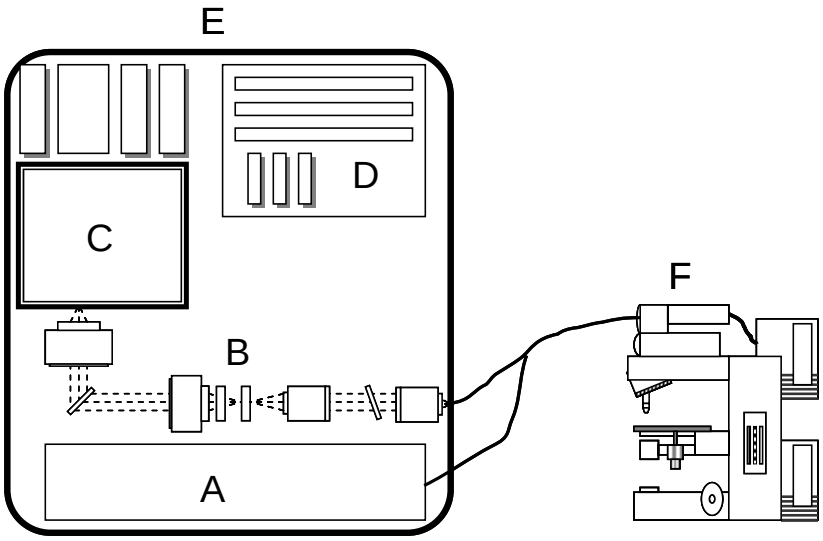

Figure 8. Schematic of Kaiser Raman Base Unit with Microprobe Attachment

Component A represents the laser. In this case, an Invictus Near IR Diode Laser was used (S/N RXN1-015). The wavelength of the monochromatic beam is 784.8 ± 0.1 nm. The output power is variable from 10-400 mW. The line width is less than 1 cm^{-1}, FWHM (Kaiser, 2001b: 9). Component B is the Raman spectrograph stage, which filters and focuses the collected light onto the detector. The spectrograph stage will be discussed in more detail in the next section. Component C represents the Charge-

Coupled Device (CCD) camera, while D is the associated camera electronics for processing the collected signals. The camera is a two-dimensional array of independent detectors, referred to as pixels, arranged on a silicon chip. The output signal from the array of detectors is serially read-out to an amplifier and processed as the Raman signal (Kaiser, 2001a: 7-11). Component F is the Raman microprobe, and is enlarged in Figure 9 (Kaiser, 2001a: 1-40).

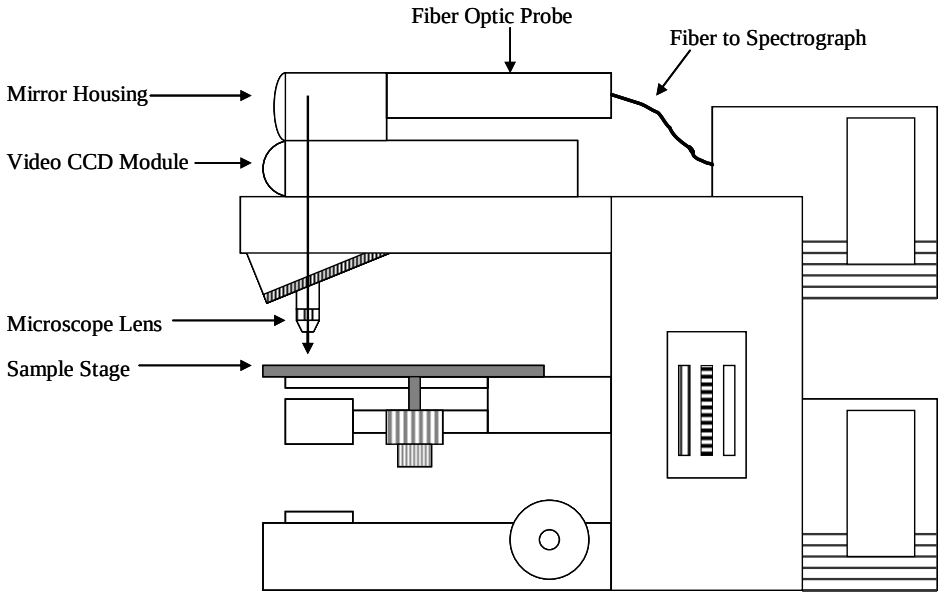

Figure 9. Simplified Schematic of Raman Microprobe

The laser serves as the source of monochromatic radiation. The beam is focused onto the sample. The back-scattered light is collected through the objective and sent to the spectrograph. The system is equipped with a video camera in the Video CCD Module. This allows the user to focus and position the laser on precisely the area of sample desired while using standard microscope eyepieces. The live video feed allows adjustment of position and focus before spectral acquisition. An image snapshot can also be taken for documentation. The use of the optical fiber for signal delivery helps to

stabilize the instrument, and eliminates the need for an optical table when mounting the microprobe.

The Spectrograph Stage. The spectrograph stage of the Raman system includes the collection optics, HoloPlex transmission grating, shutter, and slit. A simplified schematic of the whole stage system is shown in ***Figure 10*** (Kaiser, 2001a: 7-15). The collection optics includes all camera lenses and holographic optical elements included in the system. Camera lenses are used in place of mirrors because of improved aberration correction (Kaiser, 2001a: 7-14). This ultimately leads to improved spatial resolution over what is possible with a mirror system.

Once light enters the spectrograph through the fiber optic cable, it is collimated through a 50-mm, f/1.4 camera lens (L2 in the diagram). The light is sent through the notch filter (NF) and an electronic shutter (SH). The notch filter is used to reject the laser wavelength and disperse the Raman scattered light (Kaiser, 2001a: 7-14). Next the light is focused through another 50-mm, f/1.4 camera lens (L3) and onto the 50 μm spectrograph entrance slit (SL). Light which was able to pass through the slit is collimated by an f/1.8 camera lens (L4), and sent to the HoloPlex transmission grating (HG). This grating disperses and divides the collected light into a low wavenumber shift portion and a high wavenumber shift portion, then stacks the two portions on top of one another. This allows the system to have increased spectral coverage without reducing spectral resolution (Kaiser, 2001a: 7-15). The grating provides a 90º fold between the incident and diffracted light at the central wavelength. L5 is the final spectrograph focusing lens (85-mm, f/1.4 camera lens) which images the light onto the detector at the focal plane (FP).

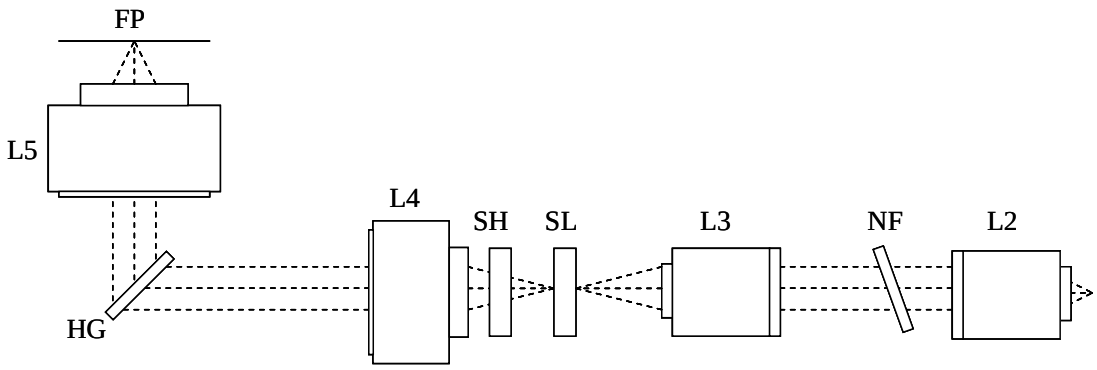

Figure 10. Spectrograph Stage of Raman Base Unit

Suitability of Raman Spectroscopy for Bacterial Investigations

Raman spectroscopy is well-suited to this biological application. It has the ability to provide spatial resolution down to 1 μm (Ferraro and Nakamoto, 1994: 172). The laser can be focused down to a pinpoint area of this size, if necessary. This is also the nominal diameter of a typical spore, so valuable information about individual members of a population could be gained using this technique. Another advantage is that it is not destructive to the biological material being measured. This was important to this study, as before and after measurements of the spores were made to gather information about viability.

There are many more applications of Raman spectroscopy related to biological studies that are beyond the scope of this document. What is highlighted are a few characteristic examples of work being done related to biological studies (mostly focusing on bacterial studies) in order to give an idea of the broad spectrum of research. Many studies can be grouped into categories of 1) exploration of molecular composition or 2) investigations into rapid identification of organisms.

In terms of investigations into the molecular composition of various organisms, Resonance Raman spectroscopy has been used to distinguish between vibrations made by the nucleic acid bases versus the aromatic amino acids of *E.coli* bacteria (Britton and others, 1988: 42). Only by using different excitation wavelengths were these differences distinguished.

Individual bacterial endospores from four species of *Bacillus* (*cereus, megaterium, subtilis, and thuringiensis)* were studied using micro-Raman spectroscopy. Spectra were dominated by scattering from calcium dipicolinate (CaDPA), with additional bands attributed to various proteins and phenylalanine (Esposito and others, 2003: 868). This technique shows promise for investigating spore to spore variability caused by such factors as environmental fluctuations.

Along those same lines, UV Resonance Raman was used to excite three species of *Bacillus* (*cereus, megaterium, and subtilis)* at various wavelengths. Spectral comparisons were made between spores and vegetative cells. Results show that excitation wavelength can be a large factor in identifying spectral differences, which are largely attributed to differences in amounts and composition of proteins and nucleic acids (Ghiamati and others, 1992: 357).

Studies have been conducted on many types of pathogenic organisms using Raman microscopy with the goal of rapid identification. One example study looked at a species of yeast, *Candida*, which has a very high mortality rate in an infected host. Early identification of the pathogen can aid clinicians to prescribe antifungal drugs. Confocal Raman microspectroscopy was able to identify 42 different strains of *Candida* after only 6 hours in culture (Maquelin and others, 2002: 594). This method shows promise for

reducing the identification time from the standard 24-48 hours down to only 6 hours with reliable identification.

Another study whose focus was rapid identification of clinically relevant microorganisms took a more general approach than Maquelin et al. Several organisms were studied by taking Raman spectra at 6, 12, and 24 hours in culture in an attempt to identify biological heterogeneity of microorganism growth reflected in the spectra (Choo-Smith and others, 2001: 1461). Organisms included *Staphyloccocus aureus, Escherichia coli,* and *Candida albicans*. Results reveal that there is very little spectral variability between replicates of the 6-hour cultures of the different organisms. 12 and 24-hour cultures, on the other hand, showed significant spectral variance which was dependent upon the depth into the colony that the spectra were taken (Choo-Smith and others, 2001: 1461). Spectra from 6-hour cultures were therefore deemed most desirable for creating a rapid identification database for classification purposes.

Infrared Spectroscopy

Accurate temperature measurements are key to generating meaningful links between heat and spore lethality. Infrared emission spectroscopy was the means by which these temperature measurements were accomplished during this research. All temperatures referenced in this research were found by analyzing IR emission spectra taken at various laser powers.

Overview of Infrared Spectroscopy. The infrared portion of the electromagnetic spectrum includes radiation of wavenumbers ranging from approximately 10 to 12,800 cm^{-1}. All objects which are at a temperature above 0 K emit infrared radiation. The

infrared radiant energy is determined by the object's temperature and surface conditions. Also, instrument response to infrared emission may be affected by atmospheric interferences and detector features. The sources of infrared radiation which are of interest in this research are black-body radiators. A black-body radiator is a surface that absorbs all radiant energy and reflects none (Meloan, 1963: 7). A perfect absorber is also considered a perfect radiator (emitter). Planck's law gives the power radiated by a black body by relating temperature of the body to the wavelength of radiation emitted by the black body (Meloan, 1963: 7). It is given by Equation 5.

$$E_\lambda = \frac{8\pi hc}{\lambda^5} \times \frac{1}{\exp(hc/kT\lambda) - 1} \tag{5}$$

where, E_λ = radiation emitted by the black body, per unit surface area per unit wavelength interval, into a hemisphere and at a wavelength λ (units are Watts/cm^2), T = temperature of the black body in ^{o}K, λ = wavelength of the emitted radiation in cm, h = Planck's constant, c = speed of light, and k = Boltzmann's constant.

When Planck's law is plotted as wavelength versus radiant emittance for various temperatures, a trend becomes clear. As temperature increases, the wavelength at which radiant emittance is at a maximum shifts to shorter wavelengths. This relationship is the basis for all temperature calculations done during this research. The wavelength at which peak radiant energy was emitted was found and related to a standard Planckian function. This function corresponded to the temperature of the blackbody radiator.

Description of the Infrared Spectrometer. A schematic of a Fourier Transform Infrared spectrometer setup similar to the one used during this research is shown in

Figure 11. A short description of the main components follows the diagram. The configuration of the IR spectrometer was never changed during this work, and all spectra were collected using this identical setup.

The laser used to excite the IR spectra was a Spectra-Physics T-Series 2 watt single-mode diode pumped Nd:YAG laser (Model IQG7600L, S/N 70522/60268). The laser frequency used during this work was 9394.5 cm^{-1}. The beam diameter is less than 1.5 mm. The HeNe laser shown in the above diagram is part of the "laser-fringe reference" system, which provides sample interval information. It also provides a "highly reproducible and regularly spaced sampling interval" (Skoog and others, 1997: 393).

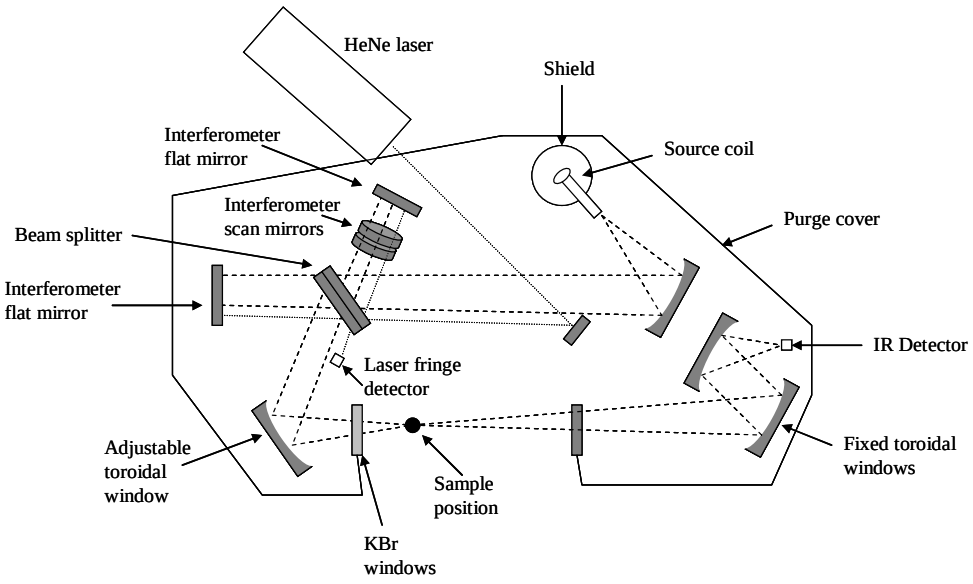

Figure 11. Simplified Schematic of a Single-Beam FTIR Spectrometer

The design of this IR spectrometer is based on the Michelson interferometer. The Michelson interferometer is used to modulate radiation in the optical region. That is to

say, the interferometer converts a very high-frequency signal to one of more measurable frequency, while maintaining the time relationships of the signal (Skoog and others, 1997: 185). The device splits the beam of radiation into two beams of almost equal power, and then recombines them in a different way so that they are of a more practical frequency that the instruments can handle.

Temperature Measurement Considerations. The spore samples were heated with a laser for a short duration of time (~ tenths of seconds to seconds). The temperature delivered to the spore itself was the quantity of interest. It proved difficult to directly measure the temperature of the spore while heating. The heat absorption in the spores themselves was not easy to measure. For this reason, heating was done indirectly by conduction/radiation from silicon-carbide (SiC). The spores were laid against a piece of SiC sandpaper during heating in order to increase the heat absorption, and therefore the peak temperature experienced by the spores. The temperature of the SiC immediately adjacent to the spore could be more easily measured, and was assumed to be a reasonable approximation to the temperature experienced by the spores. SiC was chosen for its fast thermal conductivity so that an assumption of thermal equilibrium between the spore and the material could be made.

Accurate temperature measurements were crucial to the success of this research. The amount of heat delivered to each spore sample must be precisely quantified to have meaningful neutralization data. Temperatures were calculated from the Planckian blackbody fits to corrected emission spectra, as follows: Planckian functions were fit to all data (with and without instrument/absorption response corrections), the peak

wavelength was found, and peak temperatures experienced by the spores were calculated using Planck's radiation law.

III. Methodology

Experimental Overview

This research is a new effort and does not directly build on any previous thesis project. Standard microbiology was applied to grow the organisms, but it was necessary to combine these methods with the spectroscopy in novel ways to achieve the desired results. As such, the experimental methodology was developed through professional collaboration across several scientific disciplines and a detailed literature review.

The experimental methodology was designed to exploit the advantages of both Raman and infrared spectroscopy to characterize the heating of *B. anthracis* spores. All spores were observed *in situ*, which meant under ambient conditions in the open air. *B. anthracis* was grown and sporulated in the laboratory, then mechanically washed in order to remove vegetative cell debris. The cleaned liquid spore solution was deposited on glass cover slips and allowed to air dry. Each slide was heated with a near-IR laser wavelength while an infrared spectrum was taken in order to measure applied temperature. Raman spectra of the spores were taken before and after the laser heating. The spores were then transferred to a culture plate and grown to find evidence of viability at the various heating temperatures.

The Raman return from the *Bacillus* spores is not large, so obtaining quality spectra with statistically significant counts from the bacteria depends on honing the experimental methodology to exploit all the advantages the system has to offer. Each batch of spore samples must be prepared in precisely the same manner in order to produce organisms with nearly identical characteristics at the time of examination.

The laser heating must also follow the standard procedure to ensure that each sample is heated for precisely the same time. Since this research is interested in such short timeframes, any error related to heating time may be quite significant. In addition, the protocol must be developed to ensure that all organisms on the sample experience the burst of heat. If this is not followed, the survival statistics will be skewed and meaningless.

Microorganisms

The organism *Bacillus anthracis* is the focus of this work. It was chosen because of its practical significance as a potential terrorist weapon, and availability as a pure culture.

Source. All Bacillus anthracis organisms used in this work were obtained from Dr. Eric Holwitt of the Air Force Research Laboratories, Biomechanisms and Modeling Branch, Brooks City Base, Texas. The bacteria samples began in the form of lyophilized spores from a room temperature glass culture tube. The specific strain of B. anthracis used for this research was Sterne. This is a vaccine strain of the organism. Specifically it is from a veterinary, non-encapsulated, live culture of the anthrax spore vaccine (Thraxol-2 Code 235-23). Following the Center for Disease Control regulations, all Sterne strain organisms were handled in accordance with Biosafety Level 2.

Growth. Pure cultures of Bacillus anthracis were grown from the lyophilized spores in a liquid suspension of nutrient broth over a period of ten days prior to harvesting the spores. Spores in liquid suspension were then streaked onto a prepared nutrient agar culture plate and allowed to grow for seven days before harvesting. Blank

culture plates were included in each step of the incubation to check for signs of contamination.

Nutrient broth was prepared by combining Bacto® Dehydrated Nutrient Broth (manufactured by Difco Laboratories) with water in a 500 mL glass bottle with a screw cap. The recipe for the broth was taken from the manufacturer's instructions of 8 g dehydrated broth for 1 L water. The broth solution was then sterilized in the autoclave prior to use.

All sterilizations throughout this effort were accomplished using the Tuttnaur Brinkmann 3870 autoclave. The standard procedure was 121°C at 15 psi for 15 minutes. No deviations were ever made to this sterilization procedure during this research.

To begin the growth of spores in the liquid medium, 50 mL prepared nutrient broth was transferred to a sterilized flask. A sterilized wire loop was used to transfer a small amount of lyophilized spores to the flask. The flask was loosely covered with sterilized aluminum foil and placed in the shaker incubator at 37°C and 150 rpm for 24 hours (New Brunswick Scientific C24KC Refrigerated Incubator Shaker). At this point, an additional 250 mL sterilized broth was added to the flask. The flask was again placed in the incubator at 37°C and 150 rpm and allowed to sit for 72 hours. This time allowed the bacteria to exhaust their nutrient supply and almost completely undergo sporulation. This was confirmed with a Gram stained sample from the flask.

The solution was removed and transferred to sterilized 50 mL centrifuge vials. The vials were centrifuged at 4°C and 6000 rpm for 20 minutes (Eppendorf 5810 R centrifuge). The supernatant material was poured off and disposed of, while the bacteria pellet was resuspended in 30 mL of sterilized water. The vial was vortexed to ensure

even mixing of the spore solution. Each vial was refrigerated at 4°C for 72 hours. At this point the spores were centrifuged again at 4°C and 6000 rpm for 20 minutes. The supernatant was poured off and 30 mL of sterilized water was again added. The vials were then heat shocked in a 65°C hot water bath for 35 minutes. At this point the bacteria had completed the sporulation process and were ready for sampling.

Because a highly concentrated solution of spores was necessary in order to get a strong Raman return, a culture plate of nutrient agar was streaked using a sterilized wire loop from the liquid suspension of spores and allowed to grow in the 37 ºC incubator for seven days. Nutrient agar for the culture plates was prepared by combining Bacto® Dehydrated Nutrient Agar (manufactured by Difco Laboratories) with water in a 500 mL glass bottle with a screw cap. The recipe for the agar was taken from the manufacturer's instructions of 23 g dehydrated agar for 1 L water. The agar solution was then sterilized in the autoclave prior to use. Hot liquid agar was poured into sterile polystyrene Petri dishes (Fisherbrand, 100x15mm, Cat No. 08-757-12) and allowed to cool at room temperature before streaking with bacteria. Spore harvesting from these culture plates is described later.

Gram Staining. The growth of the bacteria was characterized with the aid of a Gram staining set (Fisher Diagnostics, Cat No SG 100D). A small amount of bacteria was removed from the broth suspension using a micro-pipette (Fisherbrand Finnpipette, Ct # 21-377-328) and deposited on a glass slide. The liquid was allowed to dry, then heat fixed to the slide by passing over a flame three times.

The Gram staining was accomplished as follows: (1) apply crystal violet solution and allow to sit for one minute, then rinse gently with distilled water; (2) apply iodine

solution and allow to sit for one minute, then rinse with distilled water; (3) apply three to five drops alcohol/iodine solution, then rinse immediately with distilled water; (4) apply safranin counterstain and allow to sit for 15-30 seconds, then rinse with distilled water. This procedure is in keeping with the manufacturers instructions included with the Gram-stain application kit.

Bacilli are Gram positive organisms typically. This means that the vegetative cells should appear dark purple when undergoing a Gram stain. *B.a.* vegetative cells are no exception to this general rule. The spores, however, have very different membranes than do vegetative cells, and therefore require special staining media and techniques not used in this research. They resist normal Gram staining, and do not take up the dye. Therefore, they should appear colorless following the staining procedure, while any remaining vegetative cells should appear deep purple. One example of the gram stained organisms was shown earlier in Figure 1.

Spore Harvesting. Once the streaked culture plates had remained in the 37°C incubator for seven days, colony growth was scraped off the surface of the agar using a sterilized loop. The growth was suspended in 10 mL sterilized water. These highly concentrated spores contained some vegetative cell debris as well as broth and agar residue. It was desirable from a spectroscopic and imaging point of view to remove this residue from the spores, leaving as pure a culture as possible. The vegetative residue was removed through a series of washes and centrifugations. The vial containing the spores and 10 mL sterilized water was centrifuged at 3000 rpm and 4°C for 10 minutes. The supernatant was poured off and the spores were again suspended in 10 mL sterilized water. The vial was vortexed to ensure even mixing of the solution. The vial was then

centrifuged for a second time at 3000 rpm and 4°C for 10 minutes. The supernatant was poured off and the spores resuspended in 10 mL sterilized water. After vortexing, the vial was centrifuged for a third and final time at 3000 rpm and 4°C for 10 minutes. Once the supernatant was poured off, the spores were suspended in 3 mL sterilized water and placed in the refrigerator at 4°C to await sampling.

Spore Counting. A factor of ten dilution series was used to quantify the number of colony forming units in the final liquid spore suspension. Nutrient agar was prepared in an amount of 500 mL. The agar was placed in a 47°C warm water bath for 35 minutes. This allowed it to stabilize at a temperature cool enough so that the added spores would not be affected by the heat, yet warm enough to prevent the agar from solidifying prematurely.

In the meantime, nine sterile culture tubes were labeled with successive factors of ten from 10^{-1} to 10^{-9}. To each vial 900 μL prepared nutrient broth was added. To the first vial (10^{-1}), 100 μL of the prepared spore solution was added. This vial was vortexed to ensure even mixing. 100 μL from this first vial was added to the second vial (10^{-2}), which was then vortexed. This procedure was repeated through the remaining seven vials. From the last vial (10^{-9}), 100 μL was removed and discarded to ensure each vial contained the same amount of liquid. Once this was completed each of the nine vials contained a one tenth dilution of the previous vial. This procedure is outlined below in Figure 12.

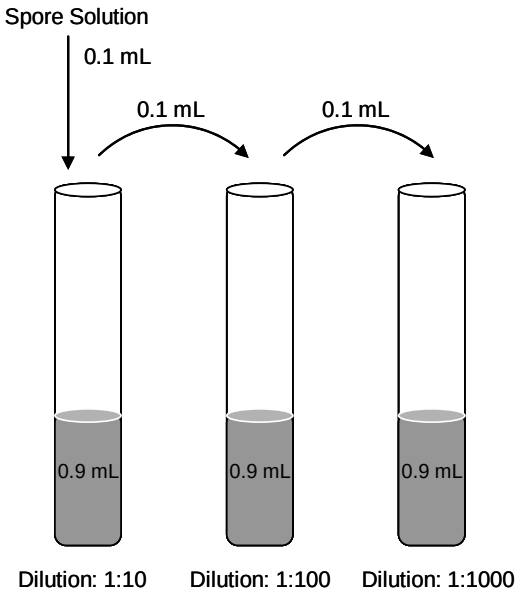

Figure 12. Use of a 1:10 dilution series

From each of the nine vials, 100 μL was taken and deposited into its own labeled sterile Petri dish. This was repeated once so that there was a replicate plate for each dilution level (18 Petri dishes total). One at a time, 25 mL warm nutrient agar was added to the Petri dishes containing the spore dilutions. The agar was swirled around to ensure even distribution of the spore liquid through the agar. Once all 18 were completed, the dishes were set aside to solidify. The solidified culture plates were placed in the 37°C incubator for 24 hours.

The colonies were counted by hand on each of the dilution plates that appeared to have between 30 and 300 spots of growth. For the replicates, the two counts were averaged. The average colony number was divided by the dilution factor and the volume of spore solution added (in mL), as shown below in Equation 6.

This quotient represents the number of colony forming units of the original spore solution. This calculation was done for each plate that appeared to have between 30 and 300 colonies. It is assumed that the calculation is accurate to the order of magnitude.

$$\frac{CFU}{mL} = \frac{\#\,colonies}{(df)(vol\ plated)} \tag{6}$$

where, df = dilution factor and vol plated = 0.1 mL. For example, if the two culture plates labeled 10^{-4} were counted as having 124 and 118 colonies, the calculation would be, $\frac{121 CFU}{(10^{-4})(0.1 mL)} = 1.21\times10^{7}\ CFU/mL$. From this, the original spore solution would be said to have approximately $1x10^{7}$ CFU/mL.

Sample Preparation

Fixing the liquid spore samples onto a suitable medium posed typical challenges from a spectroscopic point of view. First, the number of spores laid out on the slide must be great enough to generate a significant Raman return. It was desirable to have as close to a single layer of spores as possible, however, so that each spore would experience uniform heating. This would allow for the assumption that all spores in a given area were neutralized, and not just the top layer of bacteria on the slide. After some exploration, it was determined that, provided an adequate concentration of spores in the liquid solution was achieved, the liquid could simply be dropped onto a microscope slide and allowed to air dry. The proper concentration of spores was determined with visual confirmation under a light microscope (Zeiss Stemi S6 Dissecting Microscope).

Substrate. Finding an ideal substrate posed several challenges. The Raman return from the spores was very small. For this reason it was essential to choose a substrate with minimal Raman interference in the spectral region of interest. While the spores adhered very well to a standard glass slide, the photoluminescence from glass masked any Raman signal from the spores. For many of the experiments, a quartz microscope slide was instead used. The spectrum from the quartz slide alone was small in the region of interest, and spore peaks could be identified above it. The issue which arose from the use of quartz slides was their thickness. They were the same thickness as a standard glass microscope slide (1 mm). While this was fine from a spectral point of view, the microbiology of the research dictated the need for a thinner substrate. It became necessary, for reasons discussed later, for the spores to be grown up right from the slide rather than removing the bacteria and resuspending them in culture. The slide thickness needed to be such that the microscope could image through the inverted slide to the organisms below. This required the use of the very thin glass cover slips. Two substrates were therefore used during the course of the work. For primarily Raman spectral collections, the quartz slides were used, while for primarily microbiological experiments, the glass cover slips were used.

Sample Mounting. The liquid spore solution of proper concentration was mounted on the quartz slides and glass cover slips using a micropipette. The quantity varied over the course of the research depending on the specific application. Volumes dropped ranged from 0.5 μL to 5 μL over the course of the research. Slides were sterilized in an autoclave then transported to the bio hood for mounting. The spores were dropped onto the middle of the slides and allowed to dry undisturbed for an hour. Dried

slides were placed in sterile 50x11 mm polystyrene Petri dishes (Fisher Scientific 09-753-53A) for storage.

Sample Handling and Storage. All mounted samples were handled with sterilized forceps, and while wearing latex gloves, to minimize the entrance of contaminants to the sample surface. When not in use, the samples were stored in their Petri dishes at room temperature under normal humidity conditions. All samples were examined within five days of mounting. It was assumed that using the Raman system and light microscopes did not dislodge any spores from the surface of the substrate.

Raman Spectroscopy

The Raman spectrometer is well-suited to biological applications. Because the tiny spores generate such a weak signal, however, great care was taken to attempt to maximize their return. Two Raman systems exist in the laboratory. The Bomem system is the only one of the two currently configured to collect both the Stokes and anti-Stokes lines essential for temperature measurement, as discussed in Chapter 2. The collection efficiency, however, was too poor to allow adequate collection of the weak signals. The Kaiser Raman system which was ultimately used was not able to collect the anti-Stokes side of the spectrum, so only the Stokes lines were collected and used for spectral peak analysis discussed later. Raman spectroscopy for temperature measurement, although not used here, would be an ideal way to measure heat delivered to the spores, while at the same time characterizing their spectral signatures. All configuration settings and preparation steps discussed below were accomplished with the Kaiser system in order to maximize its return.

Spectrometer Configuration. The Raman system used during this work was the Kaiser spectrometer described in Chapter 2. The system was placed on top of a vibration isolation table. The experimental setup is shown below Figure 13.

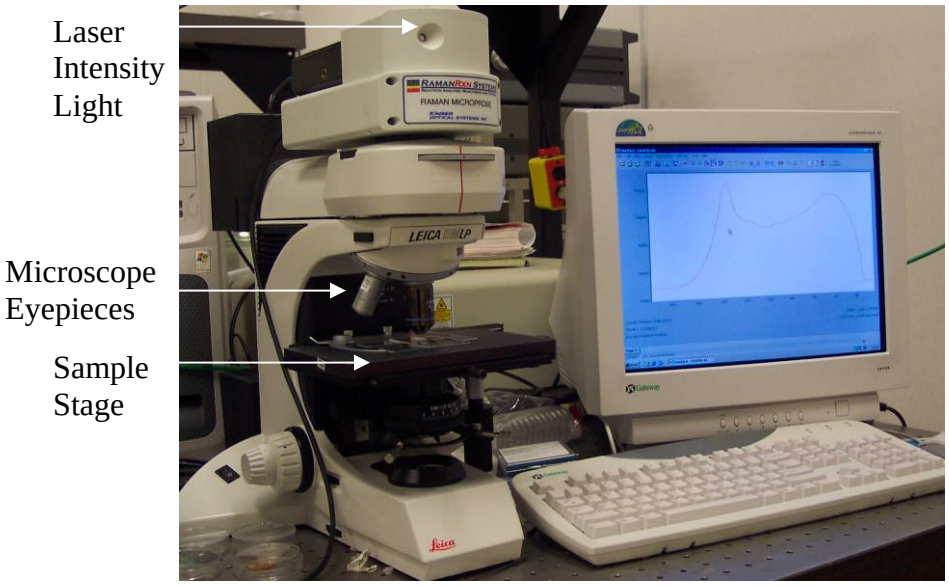

Figure 13. Photo of Kaiser Raman Spectrometer

Spectrometer Preparation. Each time the laser was turned on it was necessary to reset the laser marker using the Kaiser software. This was accomplished using a sample of a Silicon chip as a dark surface against which to see the laser spot. The laser was turned up to maximum intensity after the microscope had focused in on the surface of the Silicon. The beam spot appeared somewhat more broadened than the laser marker used by the software. The marker was set over what appeared to be the most intense area of the laser spot. Once this was accomplished, the laser intensity was lowered back to its original value.

The sample slides were placed on the Raman stage using sterile forceps. Both the quartz slides and the cover slips were too small to fit into the slide holder on the Kaiser

microscope stage. This prevented the sample from being repositioned while looking through the microscope. The slide was balanced on top of two prepositioned standard glass slides on the stage to solve this problem. The laser was still able to shine directly onto the sample, and the sample could be shifted and repositioned at will while imaging.

The laser intensity was adjusted using a screwdriver. There was no digital readout of the precise intensity at any given time. There was a small red light on the front of the instrument, as indicated in Figure 13, which would glow more or less brightly as the intensity increased or decreased. It was attempted to keep the intensity approximately the same for each spectrum taken, but this cannot be stated with absolute certainty because of the imprecise method of adjusting the laser power.

Raman Spectral Collection. Before starting the collection of a Raman spectrum, the laser needed to be positioned over an area of spores. The light microscope attachment was used for this purpose. The microscope was focused in on the sample to view the deposit of spores. An example image of the spores as they appeared under the Raman microscope is shown in Figure 14. The photo demonstrates the spores' affinity for each other. They clump together as they dry on the slide. Individual spores can be identified within the masses by their size and shape (ellipsoidal, 1-2 μm in length, 0.5-0.75 μm in diameter). The laser marker is visible as the small circle near the center of the photo. When spectra were taken, the laser marker was centered over an area of high density spores in an attempt to maximize the signal.

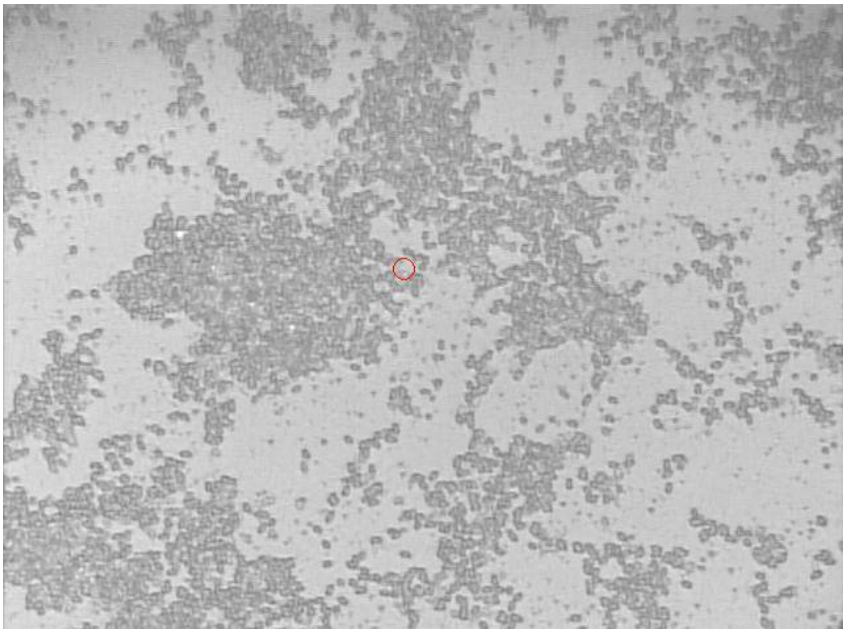

Figure 14. View of *B.a.* Spores Under through Raman Microscope

Once the collection location was chosen, the Raman system was adjusted to turn off the microscope and instead shine the laser on the prescribed sample area. Initially it was necessary to focus the laser on the sample. The Raman spectrum would refresh once every second to display the results of focal adjustments to the system. The Raman system was configured to collect the Raman shift between 0 and 2000 cm^{-1}, however at the very high end of the collection spectrum (> 1600 cm^{-1}), there was a loss in sensitivity compared to the lower part of the spectrum. The detectable features of interest in the Raman spectra of these spores lie in the shift range from 300 to 1200 cm^{-1}. It was therefore desirable to maximize this area of the spectrum with respect to all other areas. Focal adjustments were carried out in order to accomplish this. All other settings were left as selected by the computer software during the scans.

Several spectra were collected of each spore sample in an attempt to find an area displaying a more intense Raman signal. Because of optical background interferences, all spectra were collected with the laboratory room lights off. At least 50 accumulations of each spectrum were collected, and usually 75. Background spectra were collected by focusing on a blank area of the slide where spores had not been deposited and there was no visible debris. A preliminary spectrum of the spores, before heating, was always taken. After heating was completed, the after spectrum was taken using the same settings as before. These two spectra could then be compared for differences indicating changes in viability.

Sample Heating

The sample slides were heated using the Nd:YAG laser from the Bomem system. The laser diameter was approximately 250 μm. Originally the transparent slide was suspended in the sample holder and the laser was focused directly on the spores. It was discovered that even at the maximum power of 2.0 W, the absorbance of the spores was so small that they were not being heated to the point of neutralization. For this reason, silicon-carbide (SiC) sandpaper was clamped to the sample slide to increase the temperature experienced by the spores. This technique was developed for a separate experiment by Li and Burggraf in order to produce high-temperature sol-gel coatings, and was used in a similar fashion here (Li and Burggraf, 1997:258). Because the sandpaper was coarse on a microscopic level (40-100 μm particle size), the tight clamps were necessary to encourage more uniform contact between the spores and SiC. Without the

clamps, the contact between the spores and the sandpaper was very heterogeneous, as demonstrated later in Chapter IV, Figure 38.

The sample slides were placed against the SiC sandpaper using latex gloves and sterile forceps. A standard thickness sterile slide was then placed behind the sandpaper. Clamps were then attached to either end of the "slide-SiC sandwich" to hold it in place, as shown in Figure 15. The slides were too small to fit into the sample holder on the Bomem system, so the samples were suspended in the holder using the rubber band method described in the Sample Heating section above. The hood was closed over the laser and sample before any collections were taken.

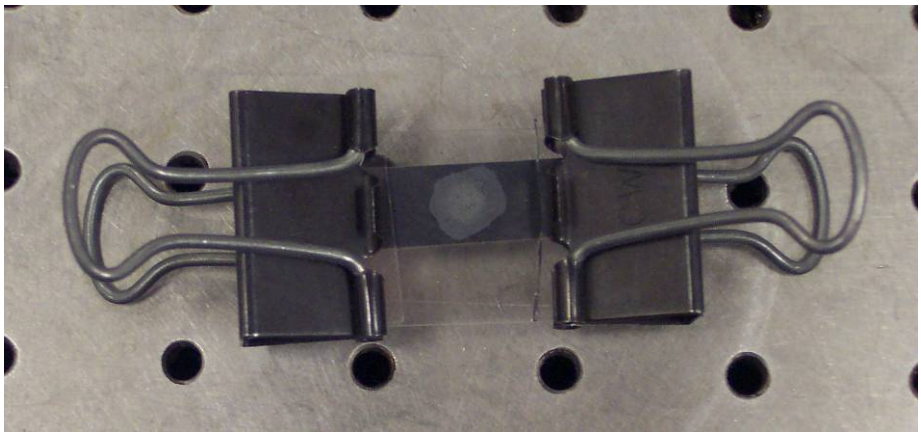

Figure 15. Spore Sample Clamped to SiC Sandpaper before Loading into Bomem

The laser controls allow for controlled movement of the sample holder in the x, y, and z directions. When heating the sample, the laser could be rastered back and forth across the spore deposit on the slide at a constant rate. In some cases one widthwise cut would be made across the spores then the laser power would be changed for another cut across the spores. The SiC demonstrated the favorable quality of keeping the applied heat very localized to the area beneath the laser track. This made it possible to examine

multiple heating temperatures on the same spore sample because only a small separation distance between cuts was necessary. The speed of rastering was manipulated using a handheld controller as shown in Figure 16. A variety of velocity settings on the controller were used for the SiC heating experiments involving rastering. Tick marks were made on the handheld controller to correspond to various rastering velocities. These are pointed out in Figure 16 with white arrows. Table 2 shows calculated velocities for the four tick marks. Heating times were calculated assuming a beam diameter of 250 μm, and range from approximately 1.2 seconds per spore for velocity 1, all the way up to velocity 4, which corresponds to about 4.2 seconds of heating time per spore.

Figure 16. Handheld Sample Stage Controller for Bomem.
Four velocity settings are marked with white arrows.

	Time to Cross 5.5 mm							
Velocity Setting	Trial 1 (sec)	Trial 2 (sec)	Trial 3 (sec)	Trial 4 (sec)	Average (sec)	Std Dev (sec)	Velocity (mm/sec)	Std Dev (mm/sec)
1	26.53	25.47	26		26.00	0.53	0.21	0.0043
2	30.82	32.06	30.16	31.25	31.07	0.80	0.18	0.0046
3	42.96	46.06	43.44	45.53	44.50	1.53	0.12	0.0041
4	92.28	108.28	94.35	106.68	100.40	8.25	0.06	0.0049

Table 2. Laser Rastering Velocity Data

Infrared Spectroscopy

The Infrared (IR) spectrometer was well-suited to aid in the measurement of applied temperature measurement during this research. Ideally the heating, temperature measurement, and spectral collection would have all been accomplished using a single Raman system. Discoveries during the course of the research, however, prevented that from being possible for this project. The collection efficiency of the Raman detector was insufficient for the weak Raman return generated by the spores. The addition of infrared spectroscopy late in the project allowed for a rough temperature measurement that was not possible otherwise with the given experimental setup. The infrared system present in the laboratory uses the same Bomem laser discussed above in the Raman Spectroscopy section. The detector in place for Raman collection was switched out and replaced with the IR detector for all temperature measurements. All configuration settings and preparation steps discussed below were accomplished with the Bomem system and IR detector in place in order to maximize its return.

Spectrometer Configuration. The IR system used during this work was the Bomem described in Chapter 2 with the DTGS detector in place. The position of the Bomem on the laboratory table was exactly as described for the Raman Spectrometer Configuration section above. The experimental setup is shown in Figure 17. The

excitation laser wavelength used in all cases was 9394.5 cm^{-1}. An expanded view of the Bomem sample collection area is shown in Figure 18.

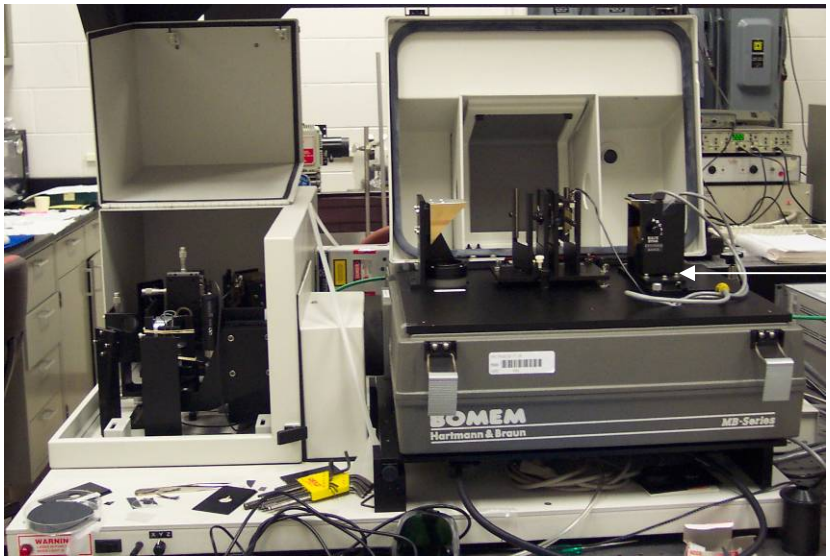

Figure 17. Photo of Bomem FTIR Spectrometer

Figure 18. Expanded View of Bomem IR Spectrometer

Spectrometer Preparation. IR spectra for temperature measurement were collected using plain SiC sandpaper without the glass cover slide containing the dried sample clamped on. There was some interference in collecting the spectra with the sample slide attached because of absorption in the glass itself. The assumption was therefore made that the closest temperature to what the spores were actually experiencing when clamped to the SiC, would be from measurements of SiC alone, without any sample attached. This removed the problem of absorption and made function fitting to identify peak location easier.

The laser intensity was adjusted using a software program on the attached computer. There was a digital readout of the precise intensity at any given time. The SiC glowed bright yellow with any laser intensity greater than approximately 0.35 W applied, indicating a very high temperature was being experienced by the SiC. If the laser was left sitting on one location of the sandpaper for a length of time, the laser would start to burn through the SiC. It was therefore desirable to complete the spectral collection quickly and turn off the laser to prevent degradation of the SiC, or if this was not possible, block the beam from hitting the sample.

Infrared Spectral Collection. Before starting the collection of an IR spectrum, the laser needed to be positioned over the desired area of SiC. This was most easily accomplished by turning the laser power up high enough to see the visible yellow glow (> 0.3 W) on an area of the SiC far away from the sample area. This allowed a visible confirmation that the laser was indeed over the SiC. Just before the laser was moved into position on the sample, the laser power was adjusted to whatever the specific collection required.

The IR system was configured to collect spectra between wavenumbers of 400 and 4000 cm^{-1}. The peaks in the spectra typically lie in the wavenumber range less than 2000 cm^{-1}. All other settings were left as selected by the computer software during the scans. Several spectra were collected of each sample in an attempt to find an area displaying the most intense IR signal. Ten accumulations of each spectrum were collected.

Spectral Analysis

The GRAMS/AI Version 7.00 software provides several analysis tools once a spectrum has been collected. Only one of them were used during the course of this research: Spectral Subtract. The Spectral Subtract algorithm was used for comparing before and after Raman spectra. Another code, courtesy of Kevin Gross, was used for fitting the Planckian functions to the data and identifying the peak location.

Planckian Function Fit. The Planckian functions were fit to the raw data using a MatLab code written by Mr. Kevin Gross. Several features in the data, both from the atmosphere and the detector system, made it challenging to get an accurate fit to the Planckian function. Modifications to the original raw data were made using Gross' algorithm, which would allow for a cleaner fit between the Planckian functions and the collected data.

First, the code was able to subtract out atmospheric features such as water lines and carbon dioxide absorption peaks from the raw data before fitting. This served to smooth out many of the larger amplitude oscillations in the data and allow for a better Planckian fit. The water and CO2 lines were matched very well by the atmospheric

corrections in the code. Second, when the detector had been calibrated, the code was able to correct for features attributable to the detector. These features lie in the smaller wavenumber side of the spectrum below approximately 1000 cm-1. This correction was helpful, but not as successful as those for the atmospheric features. The detector was calibrated assuming the following relationship:

$$R = \tau * a_1 * L(T) + a_0 \quad (4)$$

Where, R = detector response (V), L = Planckian at temperature T (W/sr-cm^2-cm^{-1}), a_1 = detector response term, a_0 = stray radiance term, τ = atmospheric attenuation factor. Given multiple T's, compute a_1 and a_0 at each frequency in least-squares.

Once corrections were made to the raw data, the Planckian functions could be fit. A least squares fit was accomplished using Gross' algorithm. The wavenumber of the peak intensity was found, allowing for temperature determinations using Planck's radiation law.

Spectral Subtract. The Spectral Subtract function of the GRAMS software does just what it sounds like. It subtracts one spectrum from another. This proved very useful for comparing before heating and after heating spectra on the Raman system. It allowed for the identification of spectral characteristics which may indicate changes in spore viability. The algorithm was used with the default software settings in each case. The only inputs added by the user were the two files to be subtracted. A typical set of two spectra and the resultant difference are shown in Figure 19. The spectral subtract was accomplished in all cases using an equation of the form:

Difference = Poly1 – (Poly2 * 1).

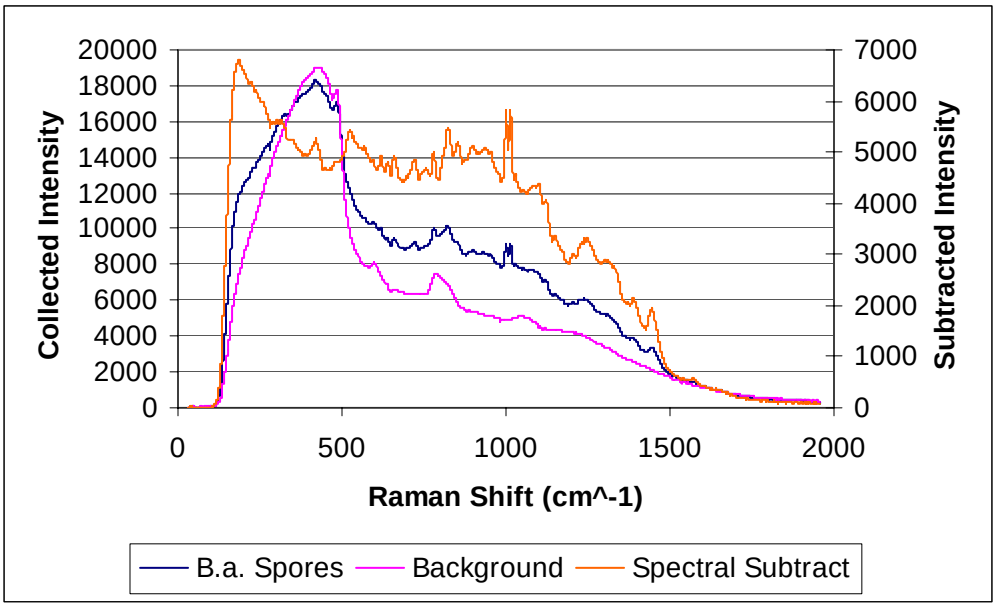

Figure 19. Example of Raman Spectra with Spectral Subtract Function

Sample Germination

Germination on Substrate. After research had begun, it was discovered that the laser diameter was small compared to the diameter of the spore deposit on the slide. The smallest volume of spores which was able to be deposited onto the slide was 0.5 μL. This volume dried to a diameter of approximately 3 mm. As the laser beam diameter was only 250 m, this meant the number of spores heated by the laser beam was small compared to the number on the slide. For this reason, instead of heating the entire spore deposit and resuspending the bacteria in culture to germinate, it became necessary to find a way to grow up the bacteria on the glass substrate. After much trial and error, a methodology was developed to accomplish this.

When attempting to grow the spores again after heating, care must be taken to ensure that as high a percentage of spores as possible come in contact with the growth

medium. Since it is presumed that the surviving spores will be few in number, it is essential for the statistical significance of the results to give as many as possible the opportunity to germinate.

A swath of spores through the deposit was heated using the laser. In most cases, the heating track was visible to the naked eye as the spores were charred and darkened in color slightly. An example of this is shown in Figure 20. A prepared nutrient agar plate from the refrigerator was left out on the countertop for a minimum of four hours in order to dry out somewhat. This allowed for the evaporation of some of the condensation that accumulates on the plates while they are stored in the refrigerator. The heated slide was to be dropped upside-down onto the prepared culture plate and allowed to grow overnight. It was discovered that any amount of water present on the surface of the agar allows the bacteria to flow somewhat from their original location on the slide while they are germinating. This is very undesirable since it is crucial that live bacteria do not flow into the area of non-viable bacteria and confuse the effectiveness of the heat treatment. The SiC sandpaper leaves a sharp gradient between heated and non-heated spores, so it was crucial to keep spores in place as they grew. The agar contains a significant amount of water, so this problem could never be entirely solved; however a workaround was devised to decrease the amount of bacteria flow. A sterile piece of absorbent filter paper (Whatman 42.5 mm circular filter papers, Cat No. 1001 042) was swabbed across the surface of the agar before laying the slide on top. This removed much of the surface water, although it did roughen the surface of the agar slightly. It was assumed that the agar surface was still coming into good contact with the spore deposit on the slide after

this was completed. This treatment appeared to decrease the flow of bacteria while germination was occurring.

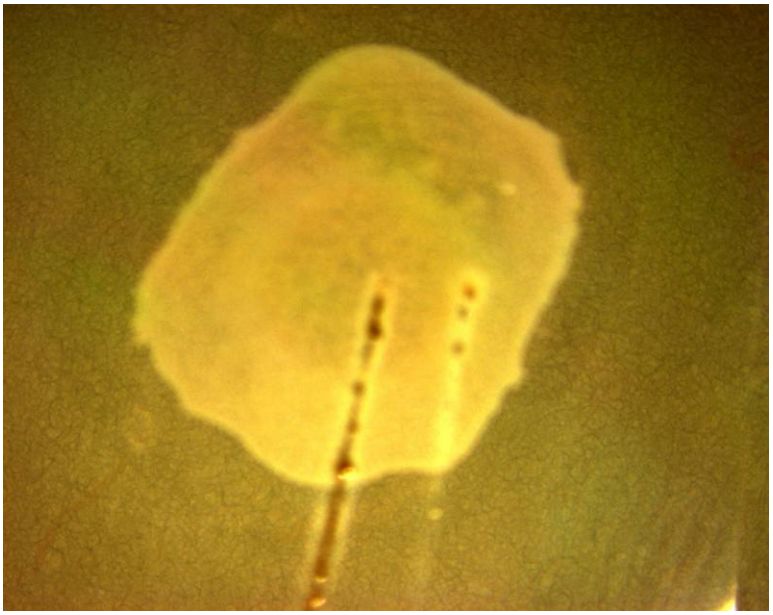

Figure 20. 0.50 and 0.35 W Laser Burn Lines through Spore Sample

Once the bacteria had been given time to germinate overnight, the entire Petri dish was studied under the light microscope. The glass cover slip was thin enough to allow the microscope to focus through to the spores up to a magnification of 400x. Because the spores were so densely packed in the deposit, it was impossible to count the number of germinating spores within the heated swath with a great amount of accuracy. Unfortunately this made statistical analysis of viability for each heating temperature impossible. All that could be done was to determine whether there was growth or no growth for a given temperature.

IV. Results and Analysis

Overview

This research resulted in the development of an experimental methodology to relate short duration heating time, temperature, and lethality measurements on *Bacillus anthracis*. Several roadblocks were encountered along the way, and evidence presented in this chapter indicates an improved approach for ensuing work. Based on these findings, the hypothesis that *B.a*. can be neutralized in very short periods of time provided the heating is intense enough has yet to be proved or disproved decisively. What was accomplished was to lay the groundwork for a more conclusive experiment which can learn from these results. As an additional goal, it was desirable to use Raman spectroscopy to attempt to characterize spectral differences in viable versus non-viable anthrax spores. A brief exploration of before and after heating Raman spectra of the spores was conducted. Further work is necessary to determine whether clear differences in certain vibrational peaks exist, indicating a change in viability of the spore. Generally speaking, results consist of Raman and Infrared spectra, photographs, and microbiological growth observations. What is missing is extensive statistical analysis necessary to generate the time/temperature profiles relating heating to spore viability.

Observations on Growth, Harvesting, and Sample Preparation

The growth, harvesting, and sample preparation proceeded as described in the Methodology chapter. None of the blank agar plates used as contamination checks showed signs of growth. One attempt at a dilution series yielded confusing results, and it was determined that the stock of nutrient broth had become contaminated. The broth was

immediately discarded, and the dilution series reaccomplished with fresh broth. The culprit was identified as a contaminated filter in the electric pipette. The filter was changed out for a clean one and no further contamination problems occurred.

The colony growth observed was characteristic of *Bacillus anthracis*. Streaked plates grown in the 37ºC incubator resulted in colonies as shown in Figure 21. The raised, grayish-white growth is consistent with the "ground glass" description usually given to these bacteria. Average colony size was approximately 3 mm in diameter.

Figure 21. Nutrient Agar Plate Streaked with *B.a*. after 24 Hours in a 37ºC Incubator

After the agar plate was streaked with the initial liquid spore prep and allowed to grow for seven days, a Gram stain was performed to check the state of sporulation. The bacteria had almost entirely sporulated, although there appeared the occasional vegetative cell. A dilution series was performed with the spores in their final liquid volume. The count came back as approximately 10^8 CFU/mL.

When dried on a glass cover slip or quartz slide, spores appeared as small dark ellipsoids against the transparent background. Any bits of debris that found their way onto the slides were easily identified as distinctly non-sporelike and eliminated from study. They did not, therefore cause confusion during the work. The *B.a*. did show a tendency to clump together in the more dilute volumes sampled. Even with vortexing immediately before dropping onto the slide, the spores would often dry together in clumps on the glass surface, as shown in Figure 14.

Raman Spectroscopic Analysis

Limited analysis was accomplished using the Raman spectra. The bulk of the research time was spent attempting to accurately characterize heating temperatures and resolving germination issues. What is included in this section is the limited spectral analysis accomplished simply to serve as a basis for any further research conducted in this area.

Several spectra were taken of each spore sample studied in the case of the Raman. There was never an indication that the spore samples were affected by the Raman scanning. The laser was kept at a low intensity, and repeated scans of the same area showed no correlated decrease in signal strength. The Raman spectra were collected with the abscissa in units of Raman shift (cm^{-1}). The ordinate in all cases is in units of arbitrary intensity. Since many accumulations were run for each spectrum, the intensity of signal represented on the ordinate is total counts through all scans.

All Raman spectra were obtained using samples of *Bacillus anthracis* from the same liquid spore volume. No differences in spore characteristics or overall density should exist between a sample slide created one day versus one created on any other day.

Raman Spectroscopy Reliability and Quality. In order to ensure the spectra obtained from one area of the spore deposit were representative of the sample as a whole, several spectra were collected of each sample. The peaks believed to be attributable to the spores demonstrated inconsistent intensity across various scans of the same sample. This is believed to be at least partially resultant from density of spores present on the slide. Because the signal from the spores is not very intense, slight adjustments to the system could result in their appearance or disappearance from the same area. Some areas of the sample deposit showed peaks while others did not.

Additionally, the machine parameters and environmental interference can have an effect on the spectra as well. The focal length from the sample was adjusted for each spectrum in an attempt to maximize the signal. Peaks appeared and disappeared simply by adjusting the fine focus on the microscope stage. Also, the optical background interference could sometimes result in a sporadic peak which could be confused with the genuine spore peaks. One such peak is identified in the spectrum shown in Figure 22. After spectral subtraction is accomplished, the background peak is the most dominant feature of the spectrum. The lights were kept very low when collecting these spectra in an attempt to remove this optical background interference.

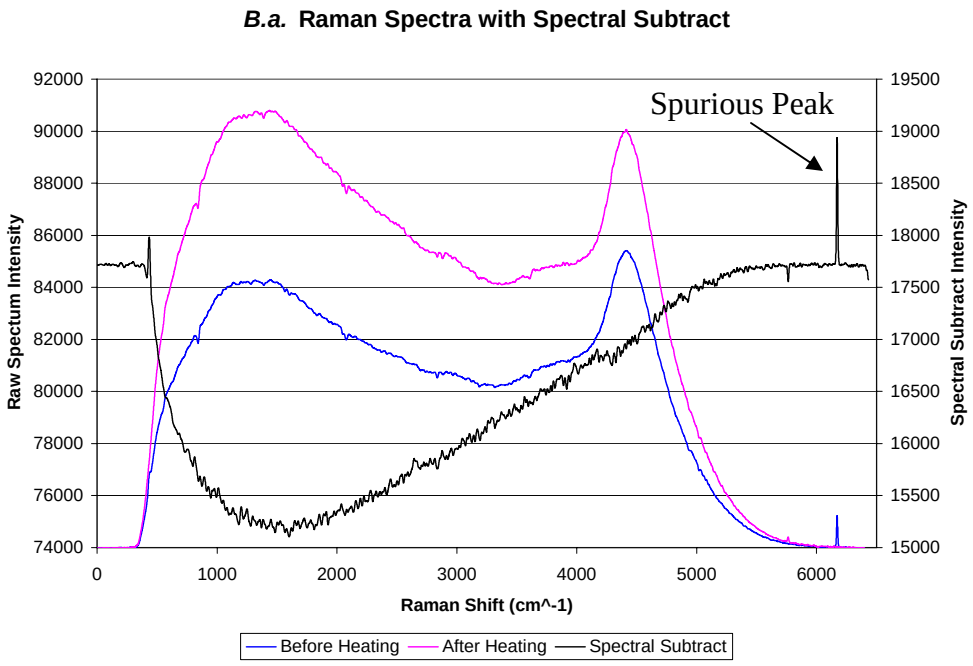

Figure 22. Example of Optical Background Interference with Raman Spectrum

After a sample was heated with the laser, the spores would sometimes be charred in appearance. When a Raman spectrum was taken of this charred area, there would be a huge amount of photoluminescence and resultant quenching experienced. The standard spectrum from the quartz or glass cover slip was totally unidentifiable beneath the luminescence. It was necessary to allow the quenching to occur for several minutes before the signal would die away and return to the characteristic signature so that the spectrum could be collected. This photoluminescence is shown in Figure 23. This spectrum was collected as a 20 scan accumulation. The peak is far greater in intensity than even the 75 scan accumulations taken of non-charred areas. This response could be attributable to polyaromatic hydrocarbons (PAH) produced by pyrolysis in the heated

samples. These molecules are fluorescent in nature, and could reasonably be responsible for the interference.

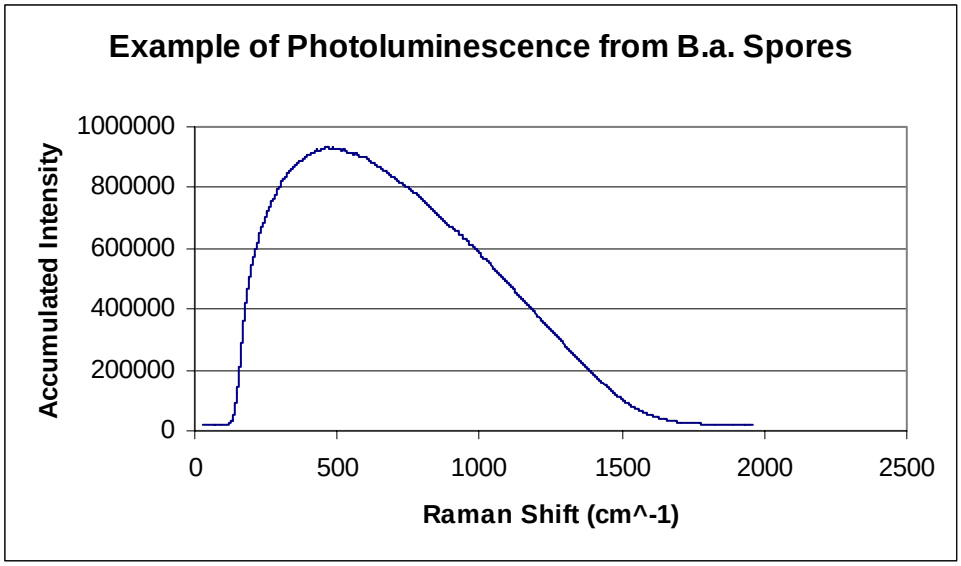

Figure 23. Photoluminescence Dominating Charred *B.a.* Raman Spectrum

Raman Spectrum Spore Information. There was one clearly identifiable feature in the spore spectra even before the background spectrum was subtracted away. This was a peak located at approximately 1013 cm-1. This peak corresponds to CaDPA in the spore coat as described by Esposito et al (Esposito and others, 2003: 868). Several other features emerge once the background quartz spectrum is subtracted away. A typical spectrum of the spores before any heating has taken place is shown in Figure 24. The CaDPA peaks are clearly visible near 1013 cm-1. The intensity of the Raman signal from the spores is not very great. The two peaks are only 411 and 113 counts above the background respectively. Other features are not quite so obvious as the 1013 cm-1 peaks. A quick comparison to Esposito et al., draws attention to other possible peaks at 822 cm-

1, 1395 cm-1, and 1445 cm-1. Each of these peaks were also attributed to the CaDPA present in the spores.

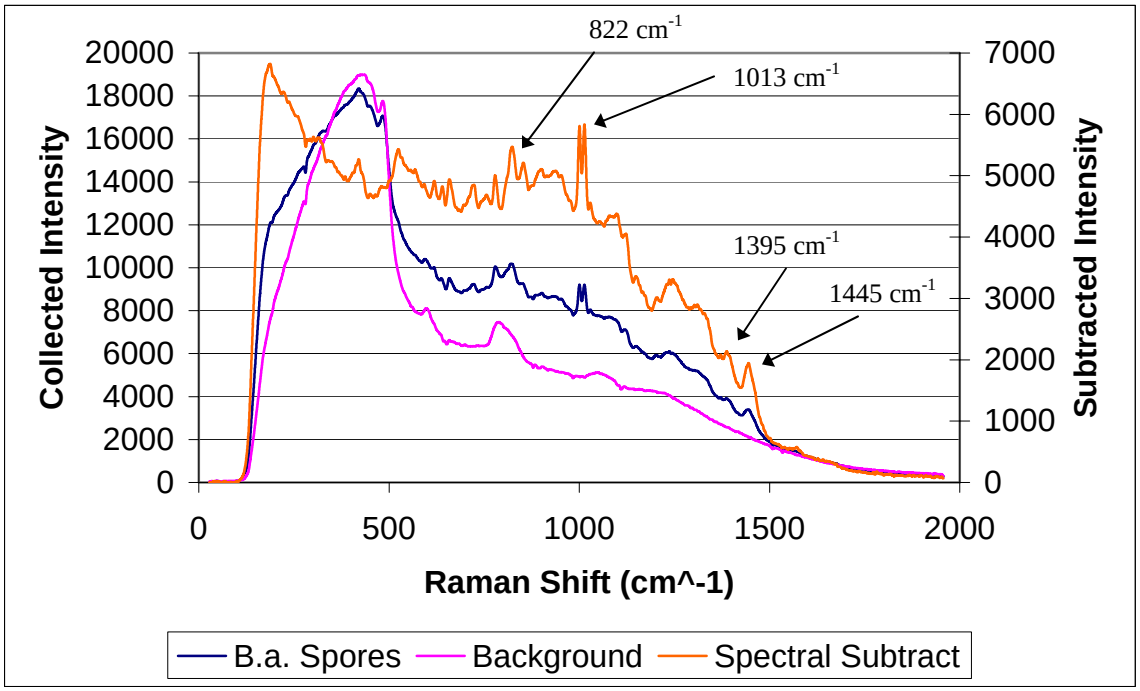

Figure 24. Raman Spectrum of *B.a.* Spores on Quartz Before Heating

No differences in the Raman spectra of before and after heated spores were visible before the SiC was attached to the samples. The spores without the SiC were not absorbing enough heat to be neutralized. After the SiC was pressed against the sample and heated, however, a change was noted in the 1013 cm^{-1} spore peaks. The charred after-spectra showed a distinct change in the magnitude of those peaks. Peak heights and areas listed in Table 3 are changes between before and after spectra measured from the spectral subtracted peaks of three different samples. The marked decrease in peak magnitude in each case may indicate that the spores underwent a structural change as a

result of the heating. The integrity of the spore coat may have been compromised by the heat so that the CaDPA is no longer intact within the spore.

Table 3. Changes in 1013 cm^{-1} Raman Peak after Heating with 0.35 W Laser

	Left Peak Area	Left Peak Height	Right Peak Area	Right Peak Height
Sample 1	5119.7	517.6	3326.0	407.7
Sample 2	4971.1	413.9	2296.4	365
Sample 3	8363.8	547.7	4222.6	563.6

Figure 25 compares a before and after heating spectrum from the *B.a.* spores. The spectral subtraction is also included. The chart is focused in on the area of interest in an attempt to make the peaks more discernable. This type of collection was made on several of the samples heated with the 0.35 W laser beam. In each case, the before spectra were collected, the samples were heated, the after spectra were collected, and a spectral subtraction was performed. Because these were the samples which were to be germinated post-heating, all slides were glass cover slips, rather than quartz. It is clear that the Raman spectrum from glass is not ideal for a sensitive study such as this. The glass background obscures the tiny spore peaks so they are much harder to discern, as compared to those seen in Figure 24.

If future work in this area focuses on Raman spectra from spores as well as heating of spores, a recommendation would be to accomplish all Raman spectral collections using quartz slides. If the slides need to be flipped upside-down onto agar for germination, quartz cover slips should be purchased and used. If that is not possible, the Raman experiments and the germination experiments should be kept separate and use two different substrate materials. Attempts to combine the two here did not result in useful Raman spectra.

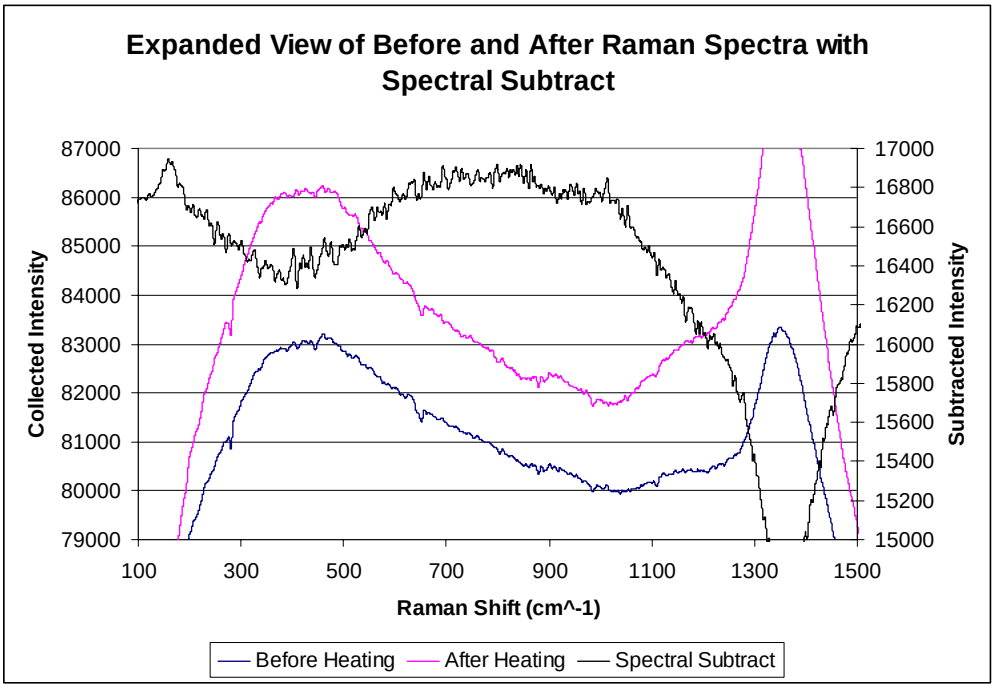

Figure 25. *B.a.* Raman Spectra on Glass Before and After Heating with 0.35 W Laser

Infrared Spectroscopic Analysis

Much of the research time was spent attempting to accurately characterize heating temperatures using the infrared spectroscopy. Difficulties arose in fitting Planckian functions to the spectra which were never entirely resolved during the course of this work. This will be discussed in detail in the following sections. Temperature estimates are provided based on the information known at the time of work completion. Further refinements of these temperatures will be necessary in follow-on work.

Several spectra were taken of each SiC sample studied in the case of the infrared emission spectroscopy. There were clear indications that the samples were affected by the laser scanning. This will be discussed in more detail below. All infrared spectra are presented with the abscissa in wavenumbers with units of cm^{-1}. This was for ease of

temperature calculation using Planck's Radiation Law. The ordinate in all cases is in units of arbitrary intensity. Since typically, several scans were run for each spectrum, the intensity of signal represented on the ordinate an average signal across all scans.

All infrared spectra were obtained using samples of SiC sandpaper cut from a larger sheet. No major differences in sandpaper characteristics (particle size, paper thickness, etc) should exist between a sample paper used one day versus one used on any other day.

Infrared Spectroscopy Reliability and Quality. It was discovered early on that the Infrared spectra being collected were sensitive to the "freshness" of the SiC sandpaper. Had the piece of sandpaper being characterized been heated previously, the emission spectra appeared to shift the location of the main spectral peak. Figure 26 shows several pieces of SiC that have undergone heating experiments. In some areas, the laser raster lines can clearly be seen, and holes where the laser burned all the way through are visible. The samples in Figure 26 were heated with no backing behind them.

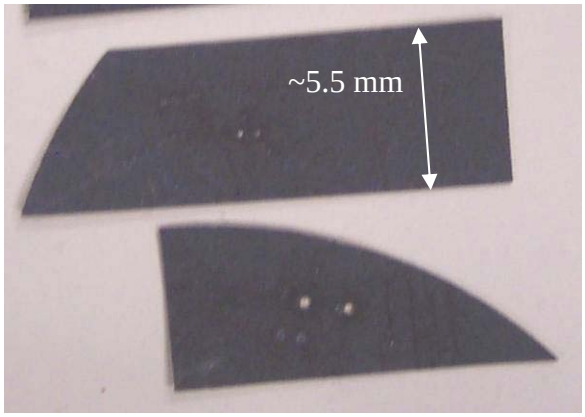

Figure 26. Visible Laser Heating Effects on SiC Sandpaper

It was therefore desirable to measure temperature on a fresh location of the SiC for each collection. This was accomplished by moving the sample holder into position immediately before collecting each spectrum. Even a few moments extra sitting on the SiC before collecting seemed to make a difference, so every effort was made to make a fresh measurement each time.

A background spectrum was taken to determine spectral contribution from non-heated areas of the SiC. An example of the background spectrum generated is shown on the same plot with a typical SiC heating spectrum in Figure 27. All spectra were taken at room temperature. It is clear that very few counts in any given heating spectrum can be attributed to background radiation. For this example the background is a factor of ten lower than the 0.35 W data in all areas.

Another check of the spectral collection was made in terms of detector response. If the detector shows an increasing or decreasing response signal through the wavelengths collected, that could affect the accuracy of temperature measurements based on the IR spectra. It was discovered that the DTGS detector exhibits a flat response through the wavelength range from 10,000 nm all the way to 200 nm as shown in Figure 28 (taken from Bomem document). Collected IR spectra did not, therefore, assume to be skewed by detector response in these experiments.

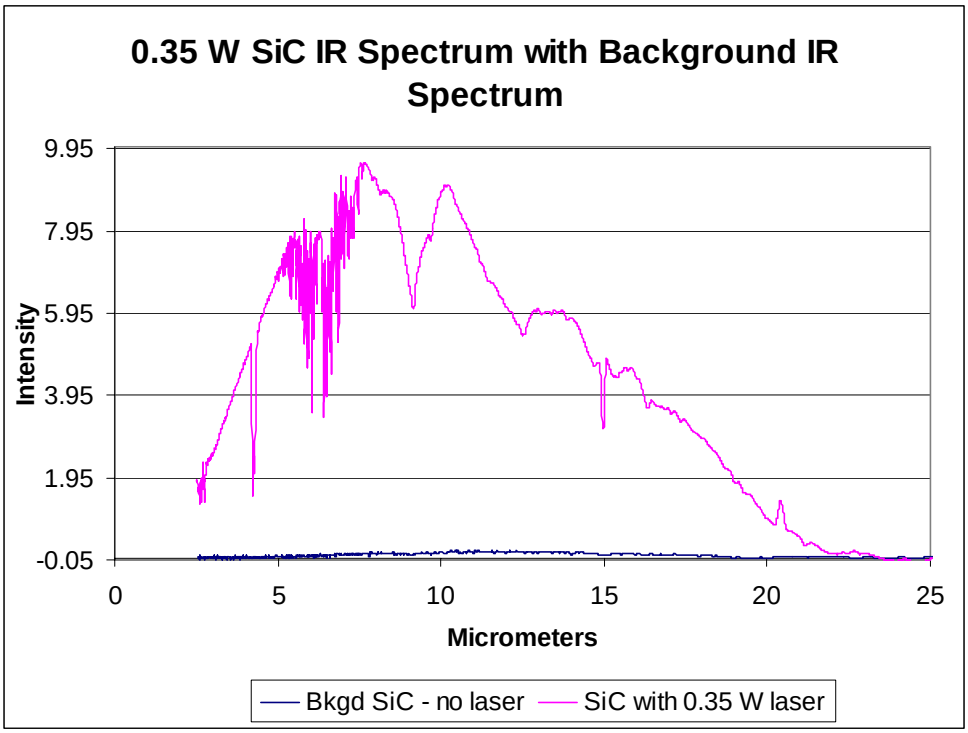

Figure 27. SiC Background Radiation in Relation to Spectrum from 0.35 W Laser

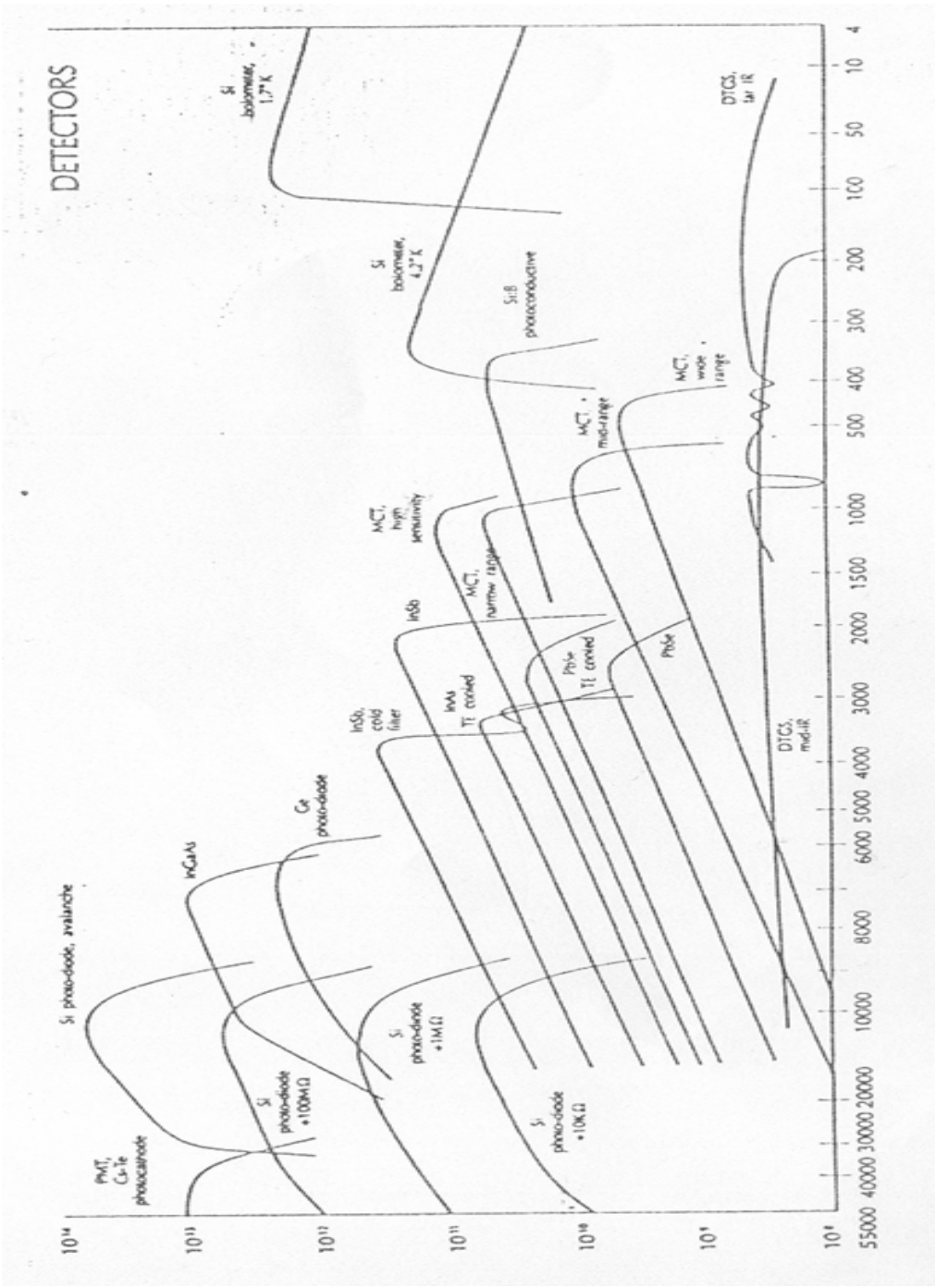

Figure 28. Various Detector Response Functions, including DTGS Detector.

Infrared Spectra and Temperature Measurements. Accurately characterizing temperature applied to the spores posed several challenges during the course of the research. These obstacles were not entirely resolved by the end of the research time. What follows are the pieces of information known at the end of the research project. Follow-on work is necessary to provide refinements in the measurements and resolve the final issues with this method.

One useful set of information was the IR calibration curves which were generated using a standard blackbody source. The source was positioned behind the empty sample holder and reflected off the parabolic mirror to the detector. Spectra of temperatures ranging from 300 K to 1200 K were collected. These spectra are shown below in Figure 29. The pattern follows exactly what is expected. As temperature increased, the wavenumber of the peak emitted radiation increased. The detector features below 1000 cm^{-1}, as mentioned above, are also clearly visible in these calibration spectra.

Much of the cause for the problems associated with temperature calculations was the fact that the laser spot size (~250 μm diameter) was small compared to the detector optics (~1 mm diameter). The detector saw an average temperature across the SiC which was a combination of the very hot laser spot and the much cooler paper surrounding this spot. Therefore, fitting a single Planckian function to a given spectrum did not accurately characterize the peak temperature experienced by the spores. Finding an accurate model to describe the radial heat diffusion outwards from the center laser spot and across the SiC proved difficult. The emittance of the SiC was not well-known, and the residue detector features tended to interfere with the fit. Since the IR spectra were typically collected at a fairly high resolution (4 cm^{-1}), the scan rate was slow (~20 scans/min). The

temperature shifting was not very clear at this detector setting. When the resolution was decreased to 128 cm^{-1} (~160 scans/min) for kinetic scan collections, the spectrum peak visibly shifted as collection time progressed. It is clear that the initial spectrum is very hot, and most likely due almost entirely to the laser spot. The later spectra indicate lower temperatures, resulting from the heat diffusion across the SiC.

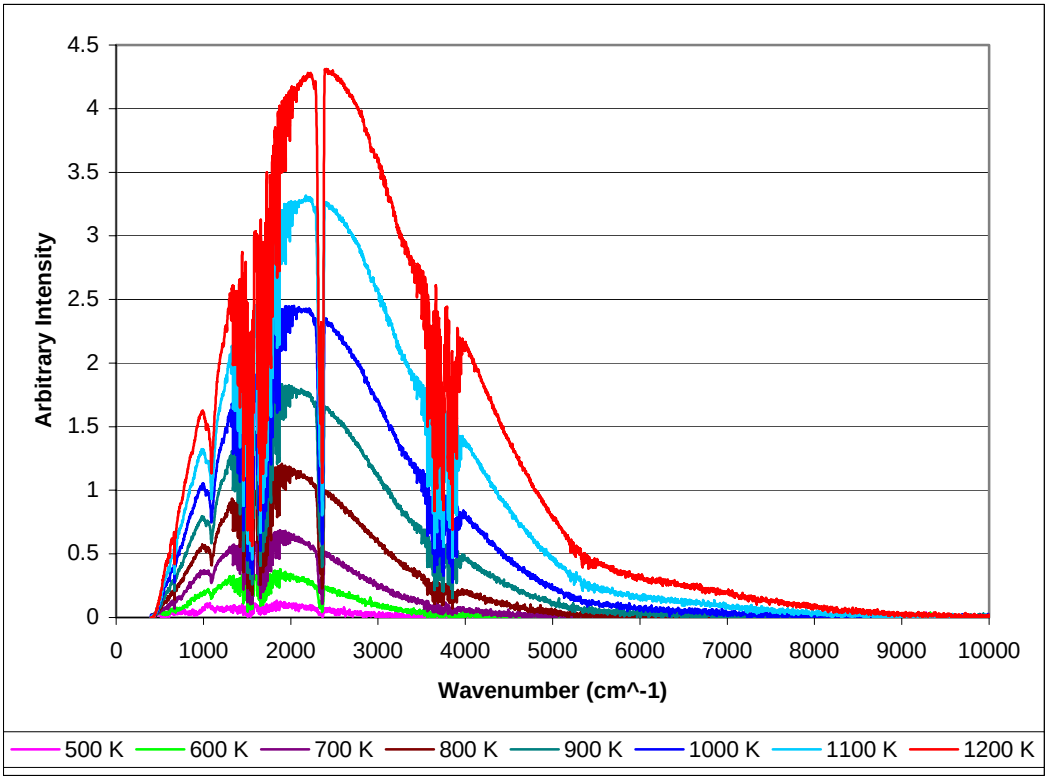

Figure 29. IR Blackbody Calibration Spectra

The heat diffusion on the SiC outwards from the laser spot was explored. Using the fast scan rate of approximately 160 scans/min, it was assumed that each scan takes approximately 0.375 seconds. Using a mean squared difference calculation, successive scans of the SiC were compared for relative change in the IR spectra. For example, the first value would be calculated by comparing the point by point differences between scan

1 and scan 2. The second value would compare scan 2 to scan 3, and so on. This data is displayed in Figure 30. This experiment was repeated three times as a redundant comparison. All three trials yielded similar results. It is clear that the SiC surrounding the laser spot heats up very quickly after the laser is turned on. After the third scan, very little change in successive IR spectra is occurring.

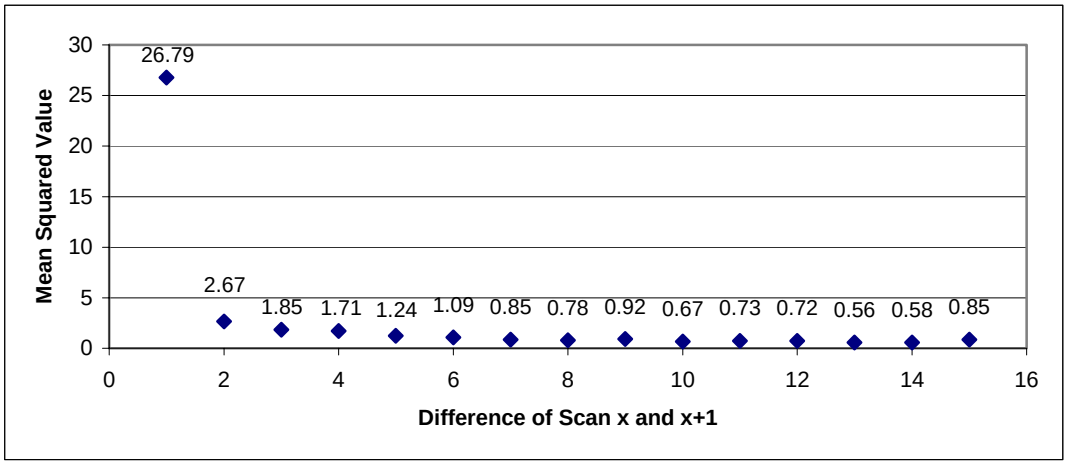

Figure 30. Mean Squared Difference Values between Successive SiC IR Scans
All scans made at laser power of 1.0 W and resolution of 128 cm^{-1}.

Since the heat from the laser diffuses radially outwards across the SiC, a range of temperatures is present along the radius collected by the detector. In order to accurately model the peak temperature, this behavior needs to be taken into account. One strategy tried was to fit two Planckians to the overall spectrum. One was a very high temperature Plackian to represent the laser spot. The other was a lower temperature function to represent the average temperature across the rest of the SiC. An example of this is shown in Figure 31. This was not very successful. The high temperature Planckian yielded temperature measurements which did not increase with increasing laser power. Also, in the spectra collected from low laser powers, the high temperature Planckian did not fit

the data well. Perhaps a better way to model this behavior would be to devise an integral which describes the heat diffusion across the radius outward from the laser spot. This was not tried during this work, but remains a possibility for the future.

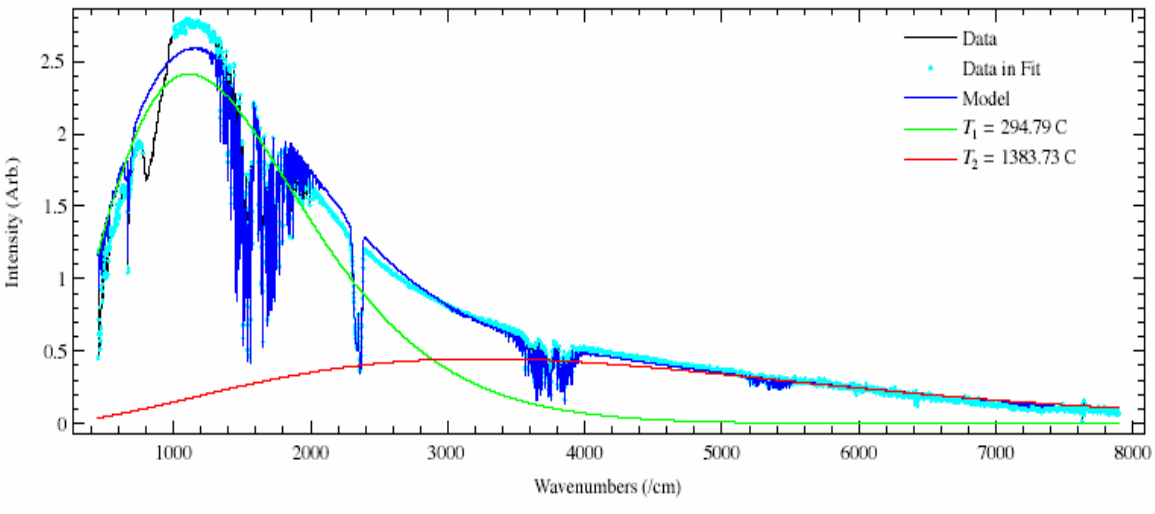

Figure 31. Two Planckian Fit to 0.40 W SiC IR Spectrum
Detector resolution of 4 cm^{-1} was used to collect spectrum. Black curve is raw data. Dark blue curve represents MATLAB model fitting raw data after atmospheric and detector corrections were applied. Green and red curves are Planckian function fits to the data.

When research time was up, this temperature issue had still not been resolved. What follows is a rough estimate of temperature for the laser powers used. As mentioned above, the first spectrum in the 128 cm^{-1} kinetic scans is assumed to be close to the laser spot temperature, since the heat has not had time to diffuse much at this point. This first spectrum was fit with a single Planckian as a rough estimate of temperature. This is shown for a 0.25 W laser beam in Figure 32. The atmosphere was corrected for using the Matlab code written by Gross. The Planckian indicates a temperature of 579.5°C. A check of this temperature estimate is accomplished with a comparison to the blackbody calibration spectra from Figure 29. The 0.25 W laser spectrum has a peak which lies near

the 500°C calibration spectrum peak, as shown in Figure 33. It was mentioned earlier that a visible glow was seen when the laser was shined on the SiC. At 0.25 W, this glow was a dull orange-red color. This would indicate a temperature in the neighborhood of ~500-600°C. All these pieces of evidence indicate that the laser beam at a power of 0.25 W is heating the spores to between 500 and 600°C.

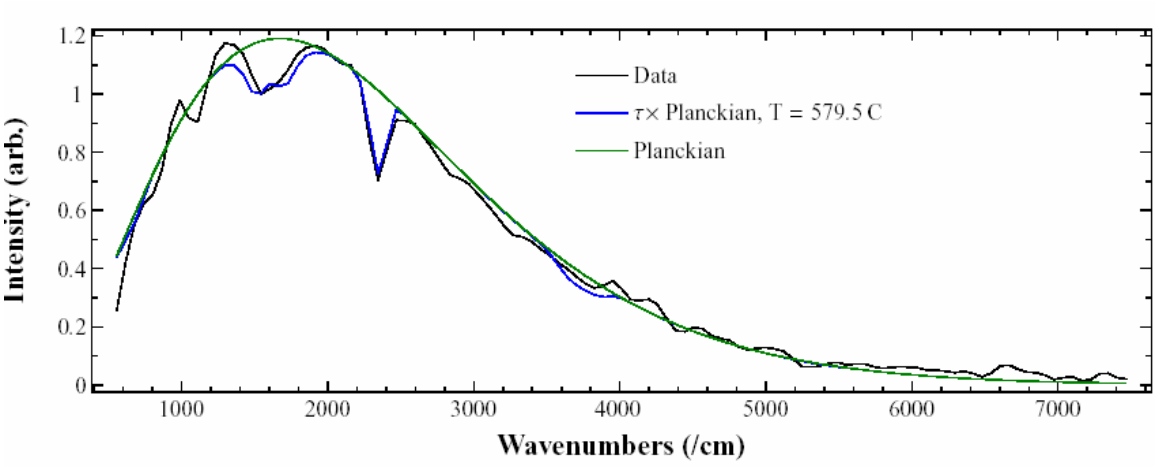

Figure 32. One Planckian Fit to First Kinetic Scan of 0.25 W SiC IR Spectrum Detector resolution of 128 cm^{-1} was used to collect spectrum. Black curve is raw data. Blue curve represents MATLAB model fitting raw data after atmospheric and detector corrections were applied. Green curve is the Planckian function fit to the data.

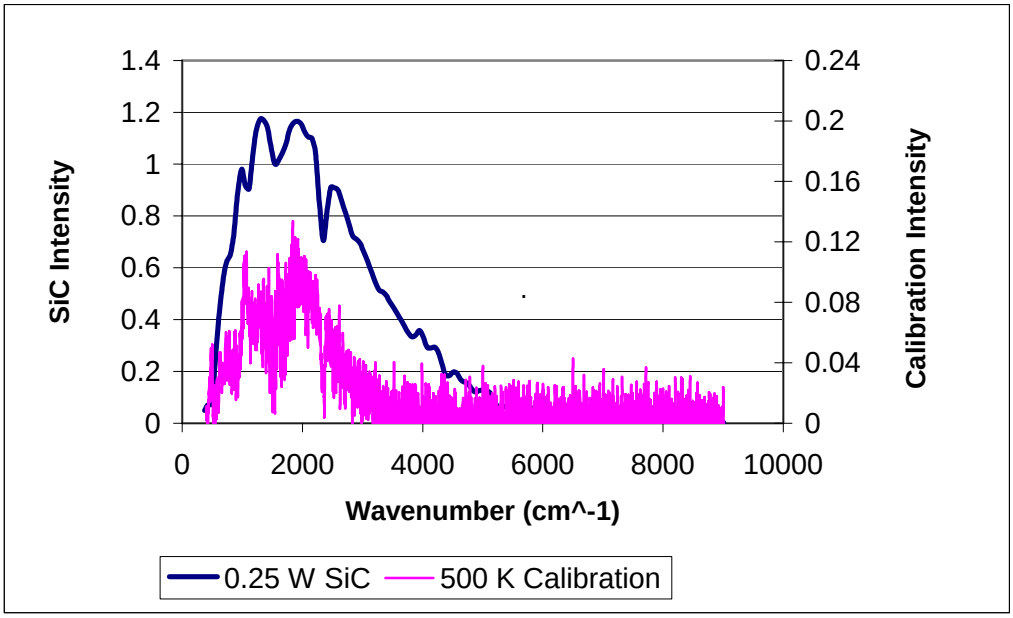

Figure 33. Comparison of 0.25 W SiC IR Spectrum to 500°C Blackbody Calibration
No background corrections are included in these curves. All data is shown in raw form.

While this method appears to work well for the 0.25 W spectra, it is less successful in estimating the temperature of the higher laser power used during the research (0.35 W). The single Planckian fit to the 0.35 W spectrum indicates a temperature of 483°C. This is lower than that calculated for the 0.25 W spectrum. Further, the 0.35 W laser gave off a bright yellow glow from the SiC. This would indicate a temperature closer to 1000°C. Figure 34 shows a comparison between the 0.35 W first kinetic scan spectrum and the closest blackbody calibration spectra. This would seem to indicate that a 0.35 W laser heats the spores to between 400 and 500°C, which is assuredly not true. This evidence supports the need for a better temperature measurement method. Perhaps the kinetic scan chosen for the one Planckian fit already included too much heat diffusion to model with a single function. Perhaps the comparison of an SiC

IR spectrum with a calibration spectrum not on SiC was invalid. It is clear that for higher temperatures, this method is not ideal.

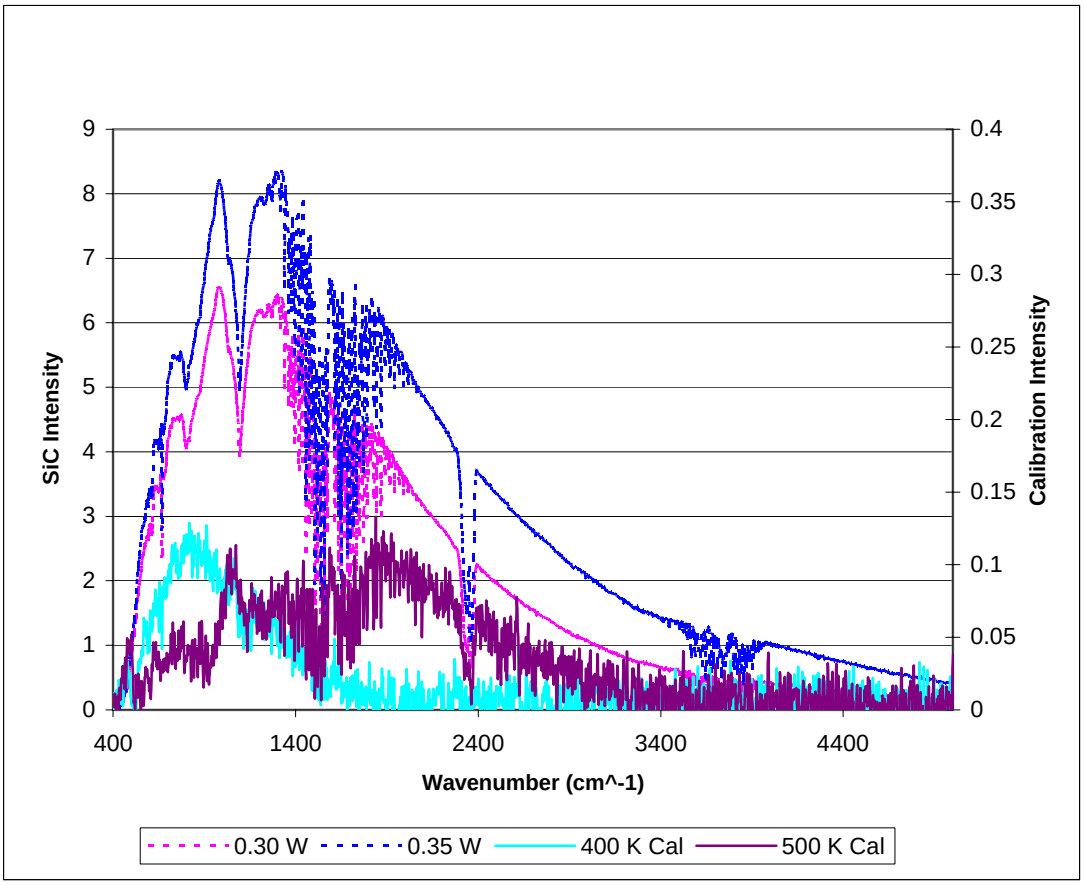

Figure 34. Comparison of 0.30 and 0.35 W SiC IR Spectra to Blackbody Calibrations

Approximating the response of the SiC as a blackbody seems reasonable from the data presented here. What needs further work at this point is how to apply the Planckian function to the collected data to yield accurate temperature measurements. It is known from the glow of the laser as it sits on the SiC that temperatures near 1000°C were being experienced at the center of the beam. This is comparable to the temperatures generated in a bomb detonation fireball of interest to this work. What is left to show is that this

temperature is accurately quantifiable by some means other than the glow of the laser spot to the naked eye.

Germination of Heated Spores

The germination of heated spores provided several challenges during the course of the research. Ultimately the method followed was to flip the heated slide spore-side-down onto the prepared nutrient agar and allow the bacteria to germinate directly from the substrate. It was essential that the bacteria stay in place on the slide when they were being grown directly from the substrate. The small amount of water on the surface of the nutrient agar allowed the bacteria to flow from their original place. This initially confused the effectiveness of the laser heating. This problem was not discovered until the SiC sandpaper was employed late in the research process. Before this point, the laser was not heating the spores enough to kill them, so the shifting of bacteria on the agar went unnoticed. Once the SiC was added and visible charring from the laser occurred, the shifting problem became apparent. Figure 35, shows a charred 0.40 W laser line after 24 hours growth time. Vegetative cells were observed in the middle of charred spores, where no growth should have been possible.

Attempts were made to swab the water off the surface using sterile filter paper. This seemed to alleviate the shifting problems and help keep the bacteria in place during the growth process. There appeared to be a sharp cutoff between live versus dead spores after the laser passed through the sample. The laser swath which would melt spores away directly beneath its trail, would leave viable spores just wide of its path. It is obvious that when trying to determine visually whether spores within the laser line were rendered non-

viable, it is extremely important for those spores outside the laser path to remain there during germination. Water is an essential part of the bacterial growth process. In this scenario, however, minimizing the freestanding water on the nutrient agar led to more accurate and interpretable growth results.

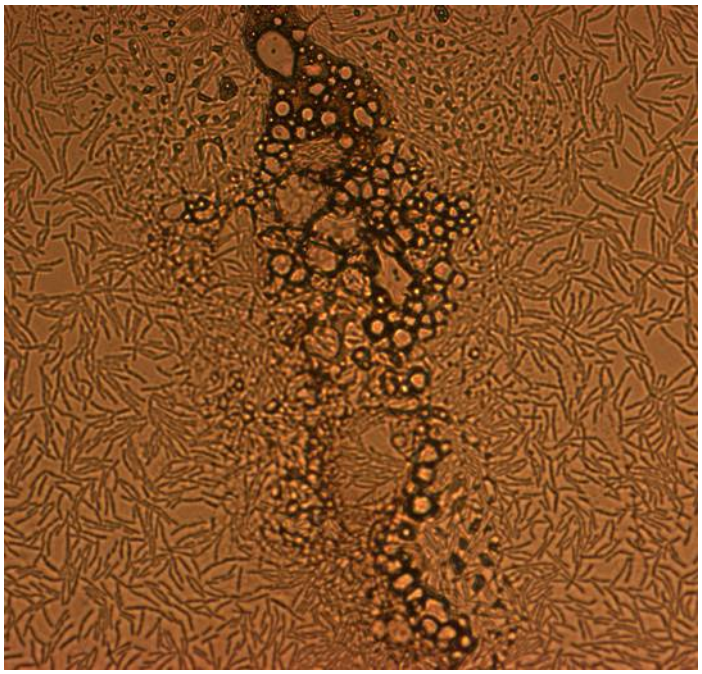

Figure 35. Evidence of Spore Shifting into 0.40 W Laser Path during Germination

Correlation of Germination and Heating

An experiment was run in an attempt to heat all the spores in a given sample deposit. The smallest volume of spores which could be deposited by micropipette onto a slide is 0.5 μL, as mentioned above. This deposit dries to a diameter of approximately 3.0 mm. The laser beam has an approximate diameter of 250 μm. This means it takes at least a dozen passes of the laser back and forth to cover the entire 3 mm diameter of the deposit. The laser was rastered back and forth across the spores to heat the entire area of dried bacteria, as represented in Figure 36. The handheld device which controls x, y, and

z movement of the sample holder is a manual control. It is difficult to ensure the platform moves precisely one laser diameter when shifting the laser down for the next pass through the sample. Every attempt was made to pack the laser tracks closely together without overlap and to cover all spore area in the deposit.

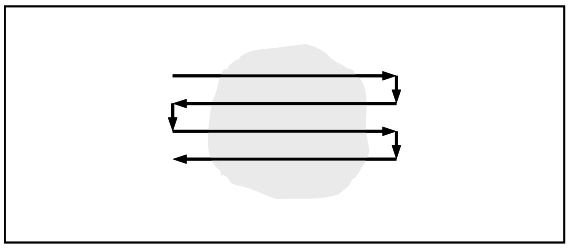

Figure 36. Depiction of Laser Rastering across Spore Deposit

A laser power of 0.35 W at the greatest velocity (setting 1) was used for the rastering experiment. Once the slide was thoroughly heated, it was transferred to a prepared nutrient agar plate for germination. The slide was inverted onto the top of the swabbed agar. The Petri dish was placed in a 28ºC incubator overnight. No signs of growth were present anywhere within the spore deposit. The Petri dish was returned to the 28ºC incubator for an additional 24 hours. Once again the plate was checked for any signs of growth. Figure 37 shows a microscope image of the plate after almost 48 hours of undisturbed germination time. It is clear that the spores which were covered by the laser rastering were rendered completely non-viable by the 0.35 W laser. No signs of vegetative cells are present in those areas. The dark clumps represent high density areas of spores and spores which discolored due to charring by the laser. The intermittent charring is another piece of evidence that contact between the spore sample and SiC sandpaper is not uniform. Heating also appears to be somewhat non-uniform because of these contact issues.

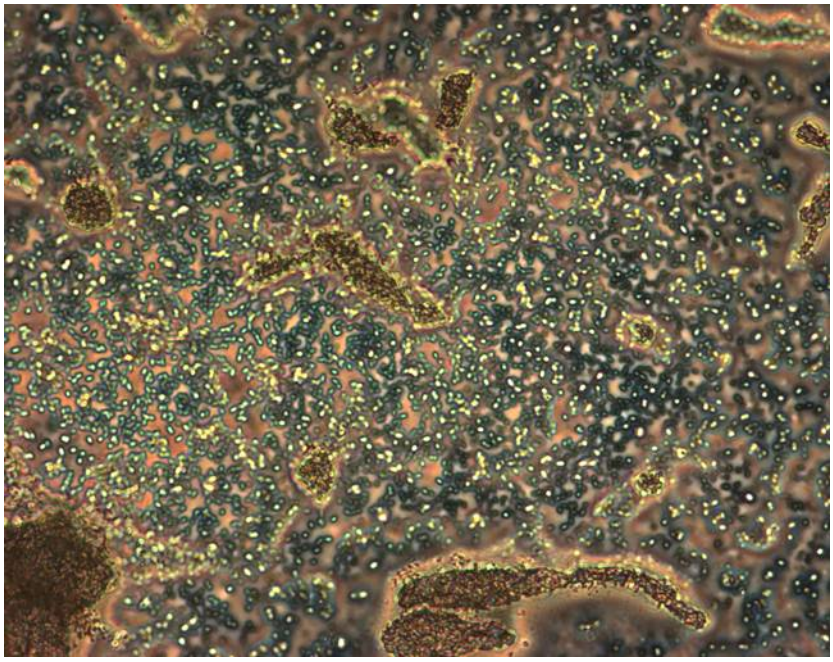

Figure 37. *B.a.* Spores Treated with 0.35 W Laser after 48 Hours in Culture Spores Appear as White or Bluish Dots.

The Effects of Varied Heating Temperatures on Germination. Several experiments were run in an attempt to correlate various heating temperatures with spore viability. Initially one slide was deposited with 5.0 L spores. The laser was rastered several times at velocity setting 1 across the spore deposit at a power level of 0.35 W. This was the same power level which was used for the burn of the entire spore area in the experiment described above. Since no growth occurred in that experiment, it is reasonable to assume that each of the burn lines in this case should show no signs of growth as well, even though not all the spores on the slide are heated. A view of a section of two of the laser lines through the sample is shown in Figure 38. The track on the right serves as a good demonstration of the intermittent contact between the SiC and the spores described earlier. Areas of good contact between the spores and SiC grains are

visible, as spores are melted away in patches where heating was very intense. Alternately, areas where the contact was less close are also visible, as spores there look virtually no different from nearby unheated spores.

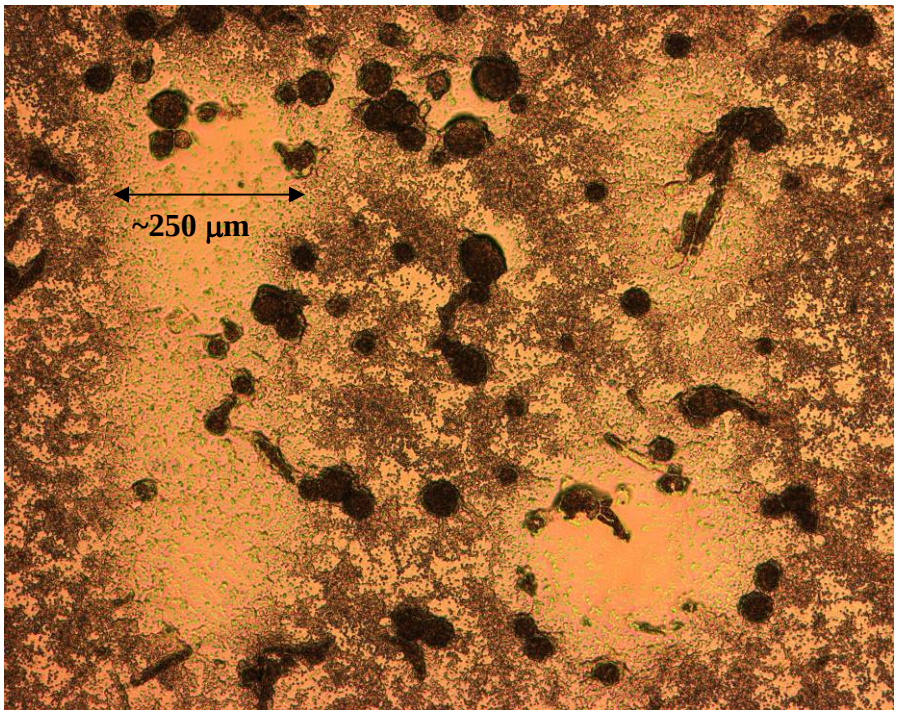

Figure 38. Two 0.35 W laser swaths cut out of a *B.a.* spore deposit at 50x magnification

Figure 39 shows results of 14 hours of germination of the bacteria surrounding one of the 0.35 W laser lines. The photo indicates that no growth has yet occurred in the charred areas of the laser path. Although obvious charring has occurred in the path of the laser, there still appear to be intact spores around the periphery of the laser path which have been rendered non-viable by the heat. Spores immediately outside the path are still viable, however, and showing signs of progressively growing into the charred area.

The Effects of Varied Heating Time on Germination. The results of Figure 37 and Figure 39 validated the ability to view viable versus non-viable spores after heating

with the laser rastering technique. This method allowed for the correlation of heating temperatures with spore viability. The next challenge was to begin to examine the heating time variable in coincidence with the temperature viability studies of the research. The next experiment again made several equal power laser cuts through a dried spore sample, but this time the laser rastering velocity was varied over each cut to change the heating time experienced by the spores.

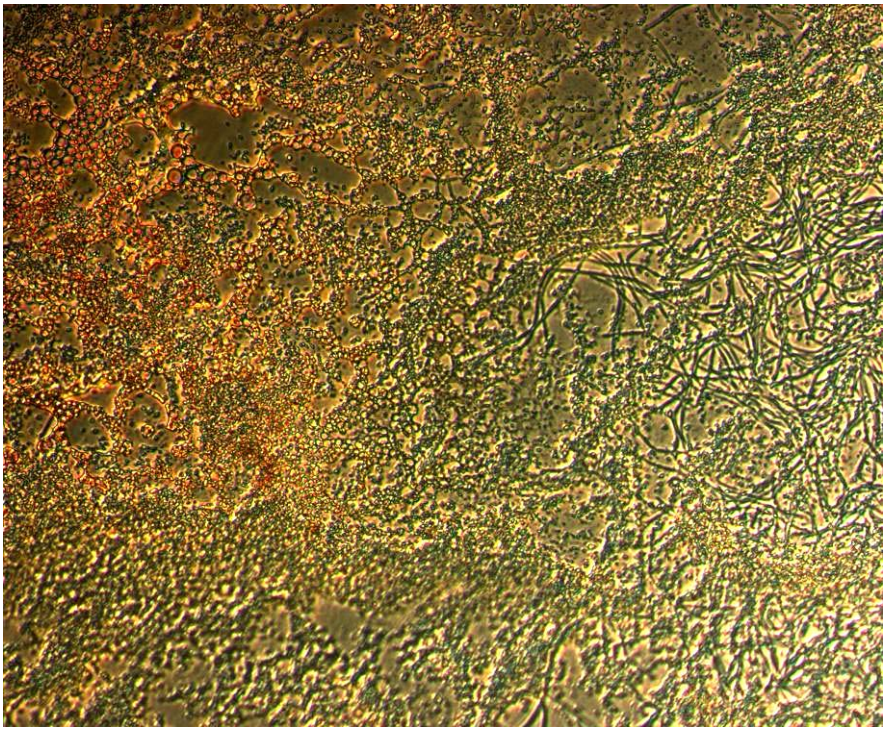

Figure 39. Growth of *B.a.* along Border of Laser Path after 14 Hours

Up until this point, the maximum rastering velocity (setting 1 in Figure 16) was used in all experiments. It was determined that at that velocity, a laser power of approximately 0.25 W did not render the spores completely non-viable. For this experiment, a laser power of 0.25 W would be used at three different velocities, corresponding to settings 1, 2, and 4 on the handheld controller. These velocities had

been previously calculated as approximately 0.21, 0.18, and 0.06 mm/sec respectively. Along with these three cuts, another cut was made with a power setting of 0.30 W and the maximum velocity. The goal of this experiment was to be able to characterize differences in germination capability at the same temperature, but with varied heating times. Photographs were taken at multiple intervals during the germination process in an attempt to characterize the growth.

Figure 40 shows a typical view of the slide immediately after being deposited face down on the nutrient agar. Spores tended to be fairly evenly distributed across the sample. Heated areas sometimes showed evidence of charring (not seen in Figure 40), however this image can be considered the time 0 state for heated and non-heated spores alike.

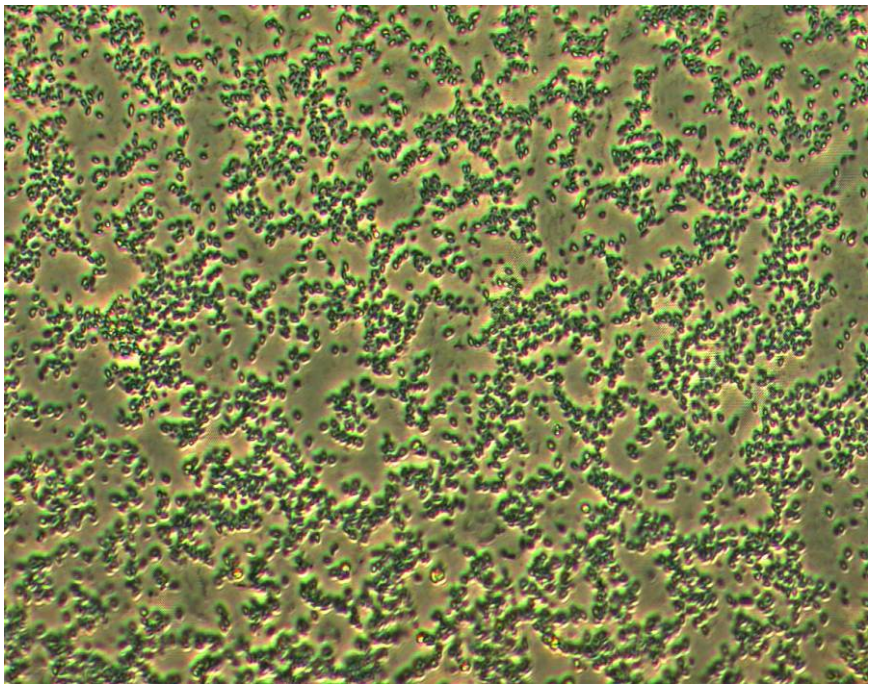

Figure 40. View of Spores Immediately after Depositing on Agar at 400x Magnification

Figure 41 shows the area of spores heated with the 0.30 W laser after 6 hours of growth time. At this point, no growth is apparent within the laser track. Some signs of germination are present on the far sides of the picture, as noted within the red circle. It is difficult to say with certainty whether this growth is within the area of spores heated by the laser track. The beam diameter is only known roughly as 250 μm from images of charred material. Additionally, temperature across the beam can be assumed to be represented by a Gaussian distribution, with spores towards the outsides experiencing slightly lower temperatures than those in the middle. This uncertainty makes it difficult to identify the heating boundaries with this method. The general lack of growth of spores obviously lying within the laser track is consistent with what was expected for this laser power and rastering speed. By way of comparison, Figure 42 shows a sample of bacteria located away from all laser lines on the slide after 6 hours of growth. Early stage vegetative cells are present and visible throughout the slide.

A rough counting analysis was conducted for comparison between Figure 41 and Figure 42. This count was accomplished using the naked eye. Both photos represent a similar field of view at 200x magnification. It was assumed that the distribution of spores was basically constant across the sample, and both figures contain a similar number of spores with equal germination opportunities. Further, it was assumed that all spores in Figure 41 were heated by the laser. While, for reasons already discussed, this is most likely not true, it was necessary in this case in order to accomplish a comparative count. In Figure 41, 5 vegetative cells were counted, while 160 were counted in Figure 42. This leads to a spore growth ratio of 1:32 for the heated versus non-heated samples. In order to make this ratio more meaningful, several replicate counts need to be made. This

calculation is included only for informational purposes and to demonstrate that rough counts are possible with this method.

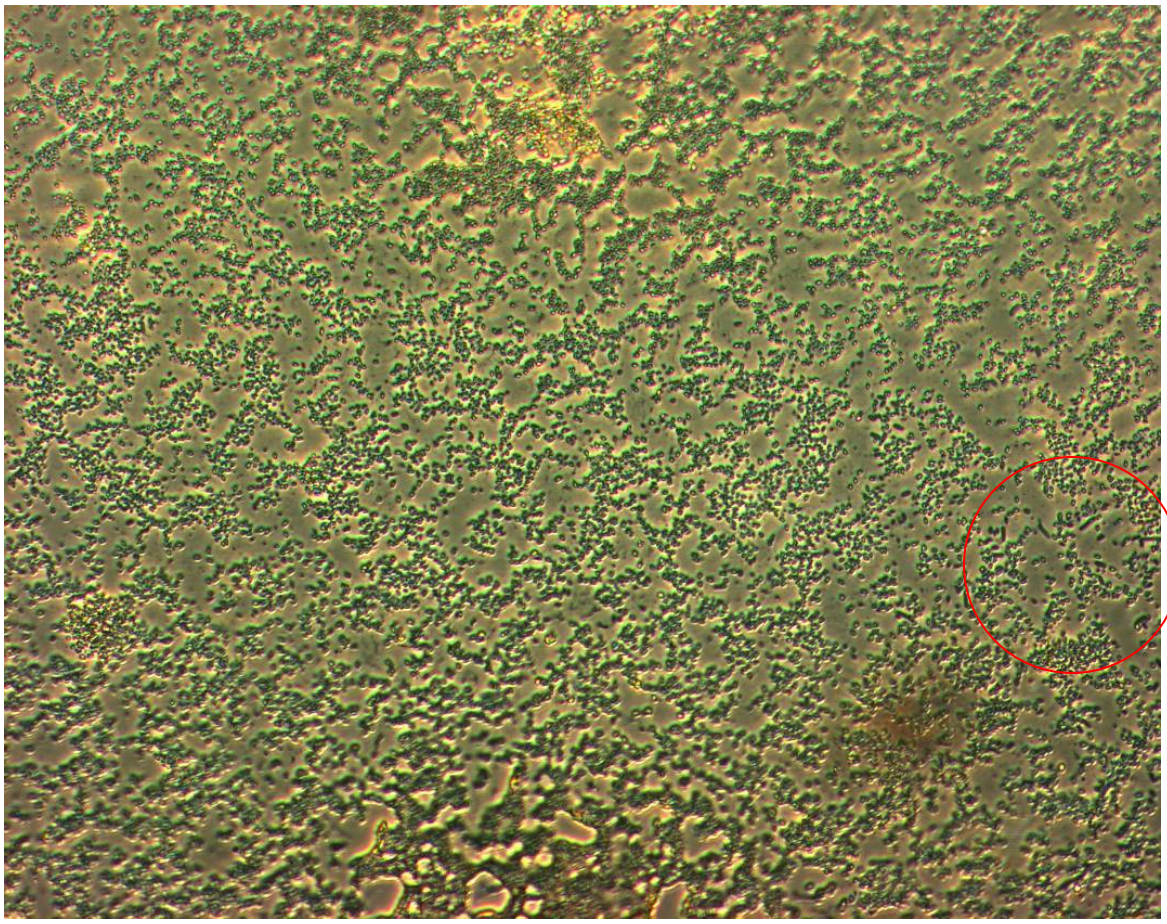

Figure 41. Growth in the 0.30 W Laser Line after 6 Hours at 200x Magnification

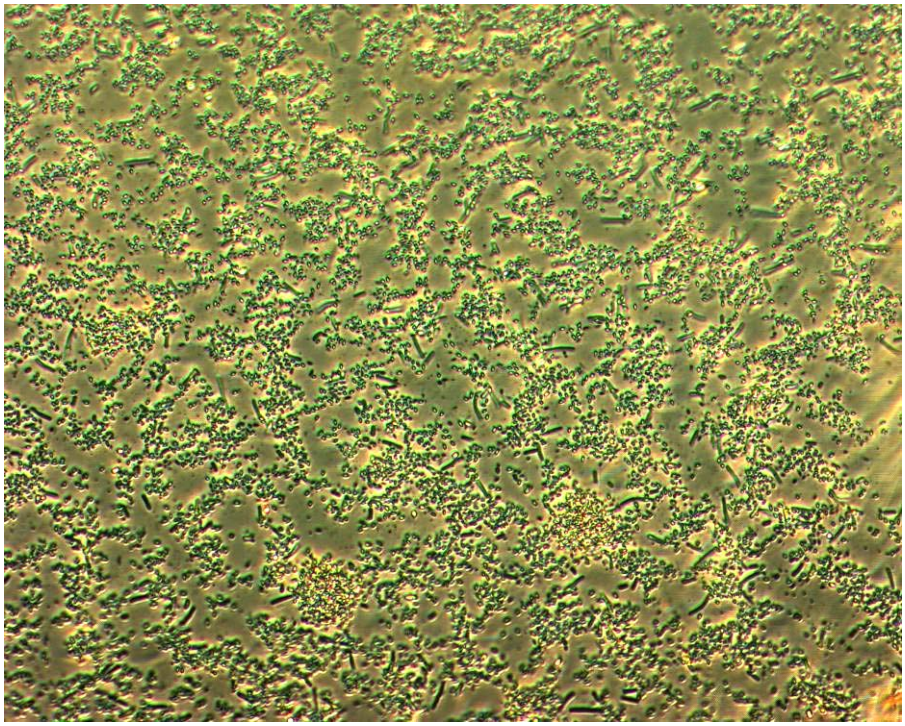

Figure 42. Growth Away from Laser Lines after 6 Hours
at 200x Magnification

By 11 hours of growth time, the scene has changed dramatically from what was shown in Figure 41 and Figure 42 above. Figure 43 shows the area of spores heated with the 0.30 W laser after 11 hours of growth time at the same 200x magnification used above. There is still no apparent growth within the obvious laser track, and the vegetative cells surrounding the track are now fully formed. The vegetative cells show signs of progressively growing in towards the non-viable spores, covering the evidence of their neutralization. Figure 44 shows the surrounding area of non-heated spores after 11 hours of growth. It is clear that this area is totally overrun with vegetative cells by this time. It appears that the viable spores immediately surrounding the laser track in Figure 43 are less numerous than those far away from the tracks (as shown in Figure 44), indicating some statistical decrease in viable spores there. This, however, is hard to say

definitively without counting analysis. The rough counting technique used for comparison above is no longer possible, as the vegetative cells are no longer distinct. They have become long chains of cells, which interweave with one another, blurring any count that would be made without a dilution technique of some sort. It may be that the initial spore deposit was simply more sparsely packed in Figure 43, however the assumption was made earlier that spore deposits were essentially uniform across the sample.

Ungerminated spores are still visible in Figure 44. Since all the spores do not germinate at the same time, this is not unusual. It does beg the question, however, whether the spores within the laser track in Figure 43 are still viable and simply delayed in their germination. Since there are clear groupings of ungerminated spores within the laser track, it is assumed that they were all rendered non-viable by the laser. It seems unreasonable that as mere chance would have it, entire clumps of spores within the track are late germinators. The more likely explanation is that they are non-viable, and will not germinate at all. It is difficult to prove this assertion photographically with this method. As a few more hours of germination time pass, the vegetative cells bordering the laser path progress inwards to meet in the middle, totally obscuring the once-visible laser track. Since no signs of germination are present within the laser track at the 11 hour point, it will be assumed that the spores were rendered non-viable there.

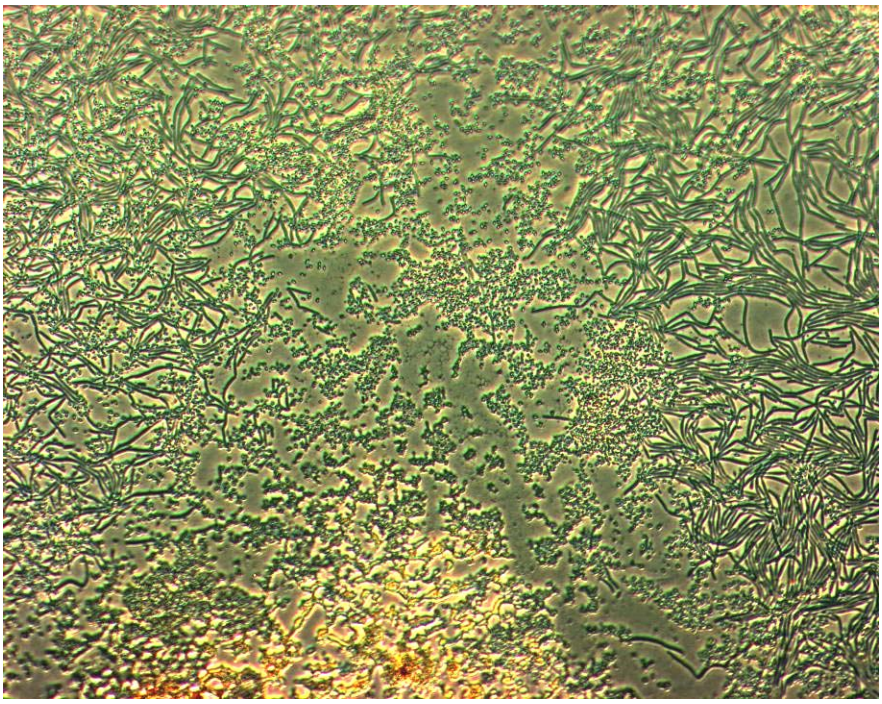

Figure 43. Growth in the 0.30 W Laser Line after 11 Hours
at 200x Magnification

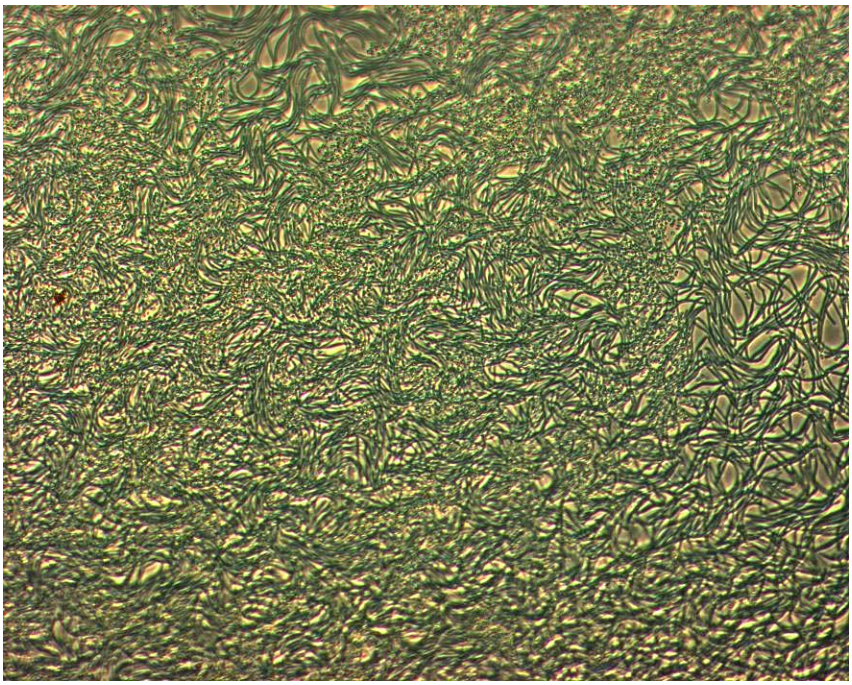

Figure 44. Growth Away from Laser Lines after 11 Hours
at 200x Magnification

With the confirmation that growth surrounding the 0.30 W laser proceeded as expected, attention can be turned to the focus of the experiment: the effects of varied heating time on lethality with the same applied temperature. In this case the 0.25 W laser was used at three differing velocities. It was discovered that velocities 1 and 2 (0.21 and 0.18 mm/sec respectively) produced results too close to distinguish by this method, so of the two, only the results from velocity 1 are reviewed here.

The results from time 0 are the same as those shown in Figure 40, and are used as the starting point for this series of photos as well. First a review of the 0.25 W laser line at the greatest velocity is made (about 1.2 seconds of heating per spore). Figure 45 shows the results after 6 hours of growth time. The early stages of vegetative cell growth are apparent. The cells in this area look very much like those in Figure 42 of the growth away from the laser track. This indicates that heating at this raster velocity had little or no effect on the cells' viability.

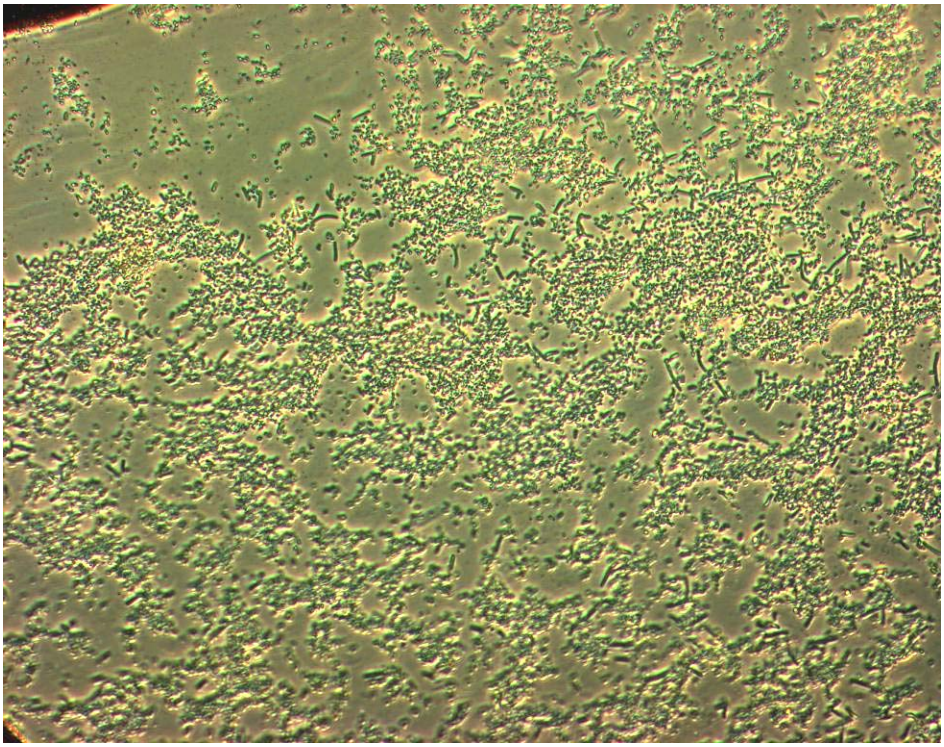

Figure 45. Growth in the 0.25 W, 0.21 mm/sec Laser Line after 6 Hours at 200x Magnification

The growth on this same laser track after 11 hours growth time is shown in Figure 46. In this case, the growth has spread uniformly through the laser line. There is no indication from the photo that the spores were heated at all. It may be ventured that the density of vegetative cells is less than that shown in Figure 44, indicating that the heating had some effect. Again, however, this is difficult to say with any certainty with this method. What is certain is a clear difference between the 0.25 W laser line and the 0.30 W laser line with the same amount of growth time.

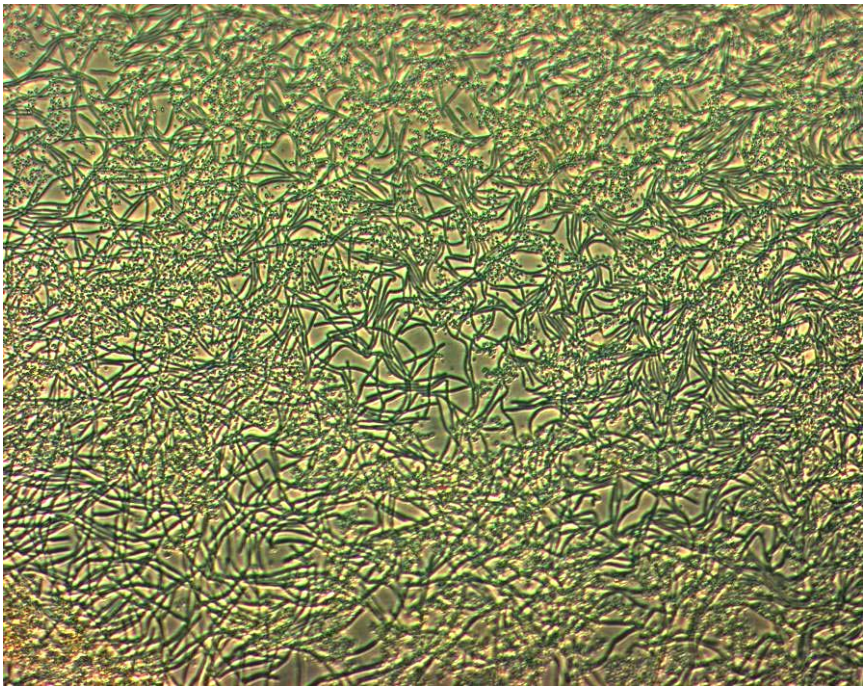

Figure 46. Growth in the 0.25 W, 0.21 mm/sec Laser Line after 11 Hours at 200x Magnification

The final review of this experiment goes to the 0.25 W slowly-rastered laser line (0.06 mm/sec and about 4.2 seconds of heating per spore). The starting point is again Figure 40, while the 6 hour photo is shown in Figure 47. Very few vegetative cells are beginning to form along the laser line at this point in the germination. Considerably fewer examples of germinating cells are present in this photo than are in Figure 45, which shows the same temperature but less heating time. This follows what is expected. At the 11 hour point vegetative cells have matured and grown in around the laser line.

A different area of the laser line is shown in Figure 48 for comparison. The vegetative cells surrounding the charred area have grown in. Note the number of spores shown in the photo which have not germinated at this point. This leads to the conclusion that some percentage decrease in overall spore viability has occurred within the laser line.

The heating was not enough to render all spores non-viable, however it was enough to be identified as responsible for a decrease in surviving spores. With this method it is difficult to quantify this decrease in viability since it is impossible to distinguish between "late germinators" and truly non-viable cells. Since examining the laser path shows such a small percentage of the total number of cells in the sample, it is hard to make decisive judgments about which spores are living and dead. The easiest way to do solve this, of course, would be to transfer the sample from the slide into a dilution series, and then allow the spores to grow culture. The statistical decrease in viability could then be calculated at the same amount of growth time for each experiment. This would require heating of the entire sample, however, which is not possible with the current experimental setup.

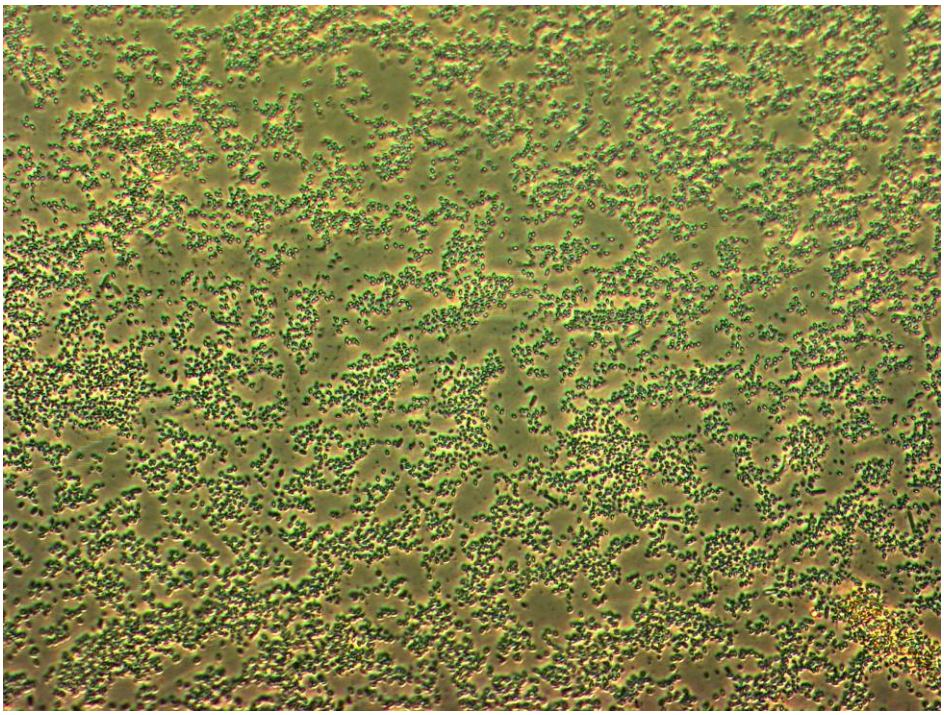

Figure 47. Growth in the 0.25 W. 0.06 mm/sec Laser Line after 6 Hours at 200x Magnification

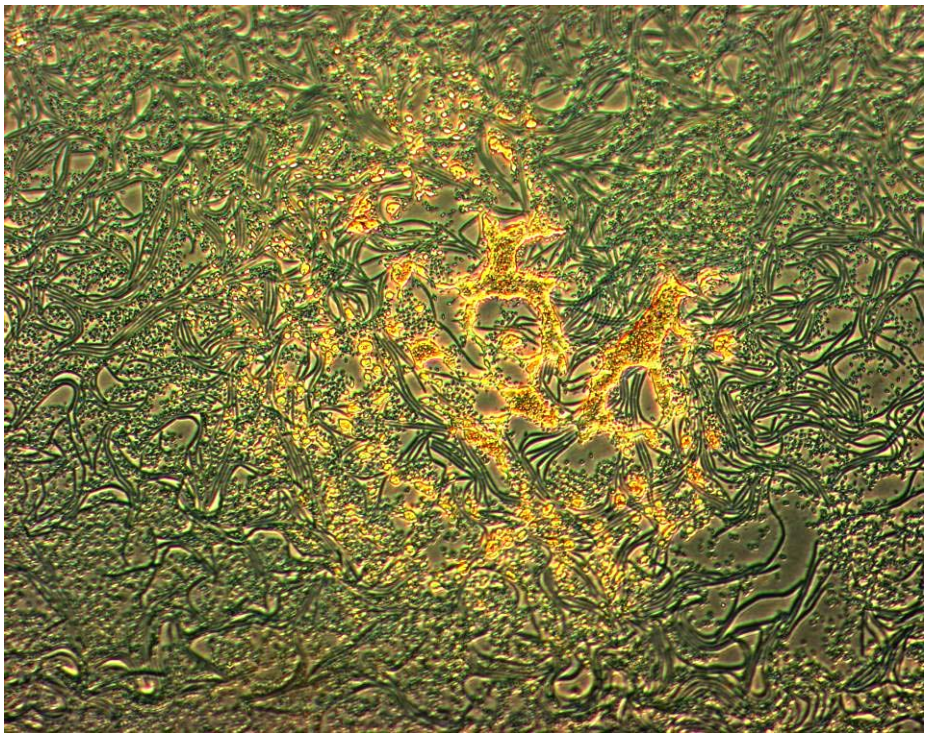

Figure 48. Growth in the 0.25 W, 0.06 mm/sec Laser Line after 11 Hours at 200x Magnification

Overall, this simple experiment served to demonstrate that there is a readily visible relationship between heating time, temperature, and spore viability. Without a better means to statistically quantify the effect on the spores, all that can be said at this point is that there was uninhibited growth, some growth, or no growth, but the relationship is still visible. One important idea that came from this is, at these high temperatures even a small change in heating time makes a great difference in spore viability. Going from a rastering velocity of 0.21 mm/sec to 0.06 mm/sec made the difference between essentially 0% lethality to an increase noticeable even without statistical counts. By conducting similar experiments and using an improved counting

method, much more can be learned about this time-temperature-lethality relationship at these short heating times.

Another important finding that came out of this experiment concerned frequency of microscope photos during germination. In Figure 48, it was difficult to determine what was happeneing since the cells had grown in so much by this point. Additional pictures taken between the 6 and 11 hour points would serve to clarify the growth process.

V. Discussion

Overview

It is clear from the limited results presented here that there is much more to learn about lethality of *Bacillus anthracis* due to short duration heating. This work is a first step on the road to this research. The main success of this work was the development of a controllable and repeatable experimental methodology upon which further research can build. The first link in the correlation between heating time, heating temperature, and spore lethality was made, but there is still a long way to go to fully characterize the effects of very short duration heat on these bacteria.

Linking Observations to Theory

The data which were collected during this research followed what was expected in terms of heating times, temperatures, and spore viability responses. Previously published literature on the subject included sparse data on short-duration heating. The vast majority of data in existence in the published literature deals with spore inactivation by long-duration heating. This longer timeframe is very well characterized within the community. The goal of this research was to fill in the shorter end of the time spectrum, using the existing data as a launching board. Projections made from the existing data were useful as an indication of threshold lethality temperatures that would be required. The research summarized in Chapter 2 indicated temperatures between 120 and 240ºC would be required for heating times of one second or less. Since the main focus of this work was to link spore viability with explosive environments created by agent defeat weapons, temperatures much higher than 240ºC were desirable during experimentation.

Laboratory simulation was able to generate temperatures near the approximate 1500K heat generated by an HE explosion. Solid links were found between the characteristic heating used here and spore death. This may be considered initial support for using a typical conventional explosion for neutralizing stockpiles of anthrax bacteria.

Recommendations for Future Work

This work was only the beginning of what can be accomplished using these techniques. The vast majority of the time spent on this research was applied towards developing a reliable and accurate experimental methodology. Challenges discovered early on proved time-consuming to overcome. When a successful correlation between time, temperature, and spore lethality was finally made, it was time to stop experimentation, and begin to summarize everything. With the procedure in place, however, the door for follow-on work is wide open.

The most obvious task which remains for follow-on work is the refinement of the temperature calculations. Rough estimations were given here by way of comparisons between collected data and a blackbody calibration source. As long as the laser beam diameter remains significantly smaller than the diameter collected by the detector, the challenge of determining temperature accurately will still exist. More work could be done to improve the code to fit Planckian functions to the IR spectra. Perhaps the radial heat diffusion on the SiC outwards from the laser beam could be modeled with an integral, rather than a few distinct Planckians. If the laser were diffused to fill the field of view of the detector, this might alleviate some of the temperature calculation problems as well.

With the method in place, a series of time/temperature profiles linked to spore lethality can now be generated. Since in the end, only two laser powers and three heating times were examined, these profiles were not generated during the course of this work. One major hurdle left in the way of accomplishing this goal is the uniform heating of an entire spore sample. This would allow the removal of the bacteria from the slide surface for resuspension in culture. Germination in this manner would allow for statistical counts to be made of live versus dead spores after each heating variation. This is the strongest recommendation for any future work related to this area. The use of a heating system which allows for a larger area of spores to be heated is highly encouraged.

In terms of current equipment limitations to accomplishing the time/temperature profiles, an alternate sample stage will need to be employed. The maximum possible raster velocity with the current stage motor was used in these experiments. This led to a heating time of approximately 1.2 seconds per spore. To reach the fraction of a second heating times which are of interest for this work, a faster stage is necessary. This time range is of importance not only because of its relationship to HE fireball lifetimes, but also from a biological damage standpoint. At long heating times the primary damage mechanism to the spores is related to chemical kinetics. As these heating times get shorter and shorter, the importance of thermal transport increases. A complete study of very short heating times is necessary to clarify this relationship.

One challenge encountered with heating the spores using the SiC sandpaper, as described in this method was uniform heating. The coarseness of the paper led to uneven heating across the laser line, as described in Chapter IV. Because of the fragility of the glass cover slips used to deposit the spores, there is a limit to how tightly the sandpaper

and the slide can be clamped together without shattering the glass. The recommendation for future experiments would therefore be to use SiC in some other form. Sandpaper with smaller particle sizes would be a slight improvement, while a smooth structure would be ideal. Since the spore deposits are small in diameter (~ 3mm), only a small chip of SiC would be necessary to complete the experiments.

It was discovered that much of the interesting vegetative cell growth begins sometime around 6 hours after addition of the nutrients. Future work might gain much insight by increasing the number of photographs taken from the 6 hour point onwards. Photos taken during this work demonstrate the stark differences between 6 and 11 hours of growth within and outside of the laser lines. Decreasing the time between photos of a specific area would be very beneficial for following the growth patterns of the viable spores as compared with those rendered non-viable by the laser.

Another variable which could be pursued in further research is the humidity factor. It is well established in microbiology that wet heat kills more effectively than dry heat. Most inactivation studies compare the lethality temperatures for types of heat. No study of short-duration heating on spores would be complete without a humidity study at those short times as well.

Spore growth environment would also make a difference in resistance to the heat. If vegetative cells undergo sporulation in a very moist environment, or a hot environment, for example, their resistance to various environmental factors can be altered. One follow-on research project could explore the effects of different growth conditions on short-duration heating of *Bacillus* spores.

Conclusions

Of the two goals of this research, progress was made on both. The primary goal was stated as developing a series of time/temperature profiles describing the lethality of *B.a.* spores. While the profiles were not generated, the experimental protocol in order to accomplish this goal was devised. No roadblocks stand in the way of this being achieved with follow-on work. The secondary goal was the exploration of spectral differences in live versus non-viable spores by Raman spectroscopy. Focus through the vast majority of this work was on achieving the primary goal. Because several obstacles were encountered in developing the experimental protocol, only a brief analysis of this phenomenon was accomplished. There is room for further analysis of this area of research as well.

Bibliography

Atlas, R.M., "Bioterrorism: From Threat to Reality," *Annual Review of Microbiology*, vol. 56, pp. 167-185, 2002.

Bagyan, I. and P. Setlow, Journal of Bacteriology, vol. 184, pp. 1219-1224, 2002.

Britton, K.A., R.A. Dalterio, W.H. Nelson, D. Britt, and J.F. Sperry, Applied Spectroscopy, vol. 42, p. 782, 1988.

Choo-Smith, L.P., K. Maquelin, T. van Vreeswijk, H.A. Bruining, G.J. Puppels, N.A. Ngo Thi, C. Kirschner, D. Naumann, D. ami, A.M. Villa, F. Orsini, S.M. Doglia, H. Lamfarraj, G.D. Sockalingum, M. Manfait, P. Allouch, and H.P. Endtz, " Investigating Microbioal (Micro)colony Heterogeneity by Vibrational Spectroscopy," *Applied and Environmental Microbiology*, vol. 67, no, 4, pp. 1461-1469, Apr. 2001.

Driks, A., "The Dynamic Spore," *PNAS*, vol. 100, no. 6, pp. 3007-3009, 2003.

Driks, A., and P. Setlow, "Morphogenesis and Properties of the Bacterial Spore," in *Prokaryotic Development.* Ed. By Y.V. Brun and L.J. Shimkets. Washington, D.C.: American Society of Microbiology, 2000.

Esposito, A.P., C.E. Talley, T. Huser, C.W. Hollars, C.M. Schaldach, S.M. Lane, "Analysis of Single Bacterial Spores by Micro-Raman Spectroscopy," *Applied Spectroscopy*, vol. 57, no. 7, 2003.

Faille, C., J.M. Membre, M. Kubaczka, and F. Gavin, "Altered ability of Bacillus cereus spores to grow under unfavorable conditions (presence of nisin, low temperature, acidic pH, presence of NaCl) following heat treatment during sporulation," *Journal of Food Protection*, vol. 65, no. 12, pp. 1930-6, Dec. 2002.

Fernelius, A.L., C.E. Wilkes, I.A. DeArmon Jr., and R.E. Lincoln, "A Probit Method to Interpret Thermal Inactivation of Bacterial Spores," *Journal of Bacteriology*, vol. 75, no. 3, pp. 300-304, 1958.

Ferraro, J.R., K. Nakamoto, *Introductory Raman Spectroscopy*. San Diego, CA: Academic Press, Inc., 1994.

Fujimori, H., M. Kakihana, K. Ioku, S. Goto, and M. Yoshimura, "Advantage of anti Stokes Raman scattering for high-temperature measurements," *Applied Physics Letters*, vol. 79, no. 7, 13 Aug. 2001.

Ghiamati, E., R. Manoharan, W.H. Nelson, J.F. Sperry, "UV Resonance Raman Spectra of Bacillus Spores," *Applied Spectroscopy*, vol. 46, no. 2, 1992.

GlobalSecurity.Org, "HTI-J-1000 High Temperature Incendiary J-1000," http://www.globalsecurity.org/military/systems/munitions/hti.htm, 2000-2004.

Kaiser, *HoloLab 5000/RamanRXN1 Operations Manual*, Michigan: Kaiser Optical Systems, Inc., 2001a.

Kaiser, *Invictus NIR Diode Laser Operations Manual*, Michigan: Kaiser Optical Systems, Inc., 2001b.

Leuschner, R.G.K. and P.J. Lillford, "Invesitgation of Bacterial Spore Structure by High Resolution Solid-State Nuclear Magnetic Resonance Spectroscopy and Transmission Electron Microscopy," *International Journal of Food Microbiology*, vol. 35, pp. 35-50, 2001.

Li, G. and L.W. Burggraf, "Laser Processing of Sol-Gel Coatings for Infrared Applications," *Proceedings - SPIE The International Society for Optical Engineering*, issue 3136, pp. 257-260, Jul. 1997.

Liu, H., N.H. Bergman, B. Thomason, S. Shallom, A. Hazen, J. Crossno, D.A. Rasko, J. Ravel, T.D. Read, S.N. Peterson, J. Yates III, and P.C. Hanna, "Formation and Composition of the *Bacillus anthracis* Endospore," *Journal of Bacteriology*, vol. 186, no. 1, pp. 164-178, Jan. 2004.

Logan, N.A. and P.C.B. Turnbull, "*Bacillus* and Other Aerobic Endospore-Forming Bacteria," in *Manual of Clinical Microbiology, 8th Ed.* Ed. P.R. Murray, E.J. Baron, M.A. Pfaller, J.H. Jorgensen, and R.H. Yolken. Washington D.C.: American Society for Microbiology, 2003.

Maquelin, K., L.P. Choo-Smith, H.A. Bruining, G.J. Puppels, H.P. Endtz, "Rapid Identification of *Candida* Species by Confocal Raman Microspectroscopy," *Journal of Clinical Microbiology*, vol. 40, no. 2, pp. 594-600, Feb. 2002.

Meloan, C.E., *Elementary Infrared Spectroscopy*. New York: Macmillan Co., 1963.

Mock, M., and A. Fouet, "Anthrax," *Annual Review of Microbiology*, vol. 55, pp. 647-671, 2001.

Molin, G., and K. Östlund, "Dry-Heat Inactivation of *Bacillus subtilis* Spores, with Special Reference to Spore Density," *Canadian Journal of Microbiology*, vol. 22, no. 3, pp. 359-363, Mar. 1976.

Orson, J.A., W.F. Bagby, G.P. Perram, "Infrared Signatures from Bomb Detonations," *Infrared Physics and Technology*, vol. 44, pp. 101–107, 2003.

Popham, D.L., J. Helin, C.E. Costello, and P. Setlow, "Muramic Lactam in Peptidoglycan of *Bacillus subtilis* Spores is Required for Spore Outgrowth but not for Spore Dehydration or Heat Resistance," *Proceedings of the National Academy of Sciences*, vol. 93, pp. 15405-15410, Dec. 1996.

Rosovitz, M.J., M.I. Voskuil, and G.H. Chamblis, "Bacillus," in *Topey and Wilson's Microbiology and Microbial Infections*. Ed. L. Collier, A. Balows, and M. Sussman. New York: Oxford University Press, 1998.

Setlow P. and E.A. Johnson, "Spores and Their Significance," in *Food Microbiology: Fundamentals and Fronteirs*. Ed. M.P. Doyle, L.R. Beuchat and T.J. Montville. Washington, D.C.: ASM Press, 2001.

Skoog, D.A., F.J. Holler, and T.A. Nieman, *Instrumental Analysis, 5th Ed*. Thomson-Brooks/Cole, 1997.

Spectra-Physics, *T-Series Laser System Preliminary Instruction Manual*, California: Lpectra-Physics Lasers, Inc., 1996.

Spotts-Whitney, E.A., M.E. Beatty, T.H. Taylor, Jr., R. Weynant, J. Sobel, M.J. Arduino, D.A. Ashford, " Inactivation of *Bacillus anthracis* Spores," *Emerging Infectious Diseases*, vol. 9, no. 6, Jun. 2003.

Willet, H.P. "Bacillus," *Zinsser Microbiology*. W.K. Joklik, H.P. Willet, D.B. Amos, and C.M. Wilfert. Norwalk, CT: Appleton & Lange, 1992a.

Willet, H.P. "Physiology of Bacterial Growth," *Zinsser Microbiology*. W.K. Joklik, D.B. Amos, and C.M. Wilfert. Norwalk, CT: Appleton & Lange, 1992b.

REPORT DOCUMENTATION PAGE

Form Approved
OMB No. 0704-0188

PLEASE DO NOT RETURN YOUR FORM TO THE ABOVE ORGANIZATION.

1. REPORT DATE *(DD-MM-YYYY)*	2. REPORT TYPE	3. DATES COVERED *(From - To)*
21-03-2005	Master's Thesis	Jun 2004 - Mar 2005

4. TITLE AND SUBTITLE

LETHALITY OF BACILLUS ANTHRACIS SPORES DUE TO SHORT DURATION HEATING MEASURED USING INFRARED SPECTROSCOPY

5a. CONTRACT NUMBER

5b. GRANT NUMBER

5c. PROGRAM ELEMENT NUMBER

6. AUTHOR(S)

Goetz, Kristina M., Captain, USAF

5d. PROJECT NUMBER

5e. TASK NUMBER

5f. WORK UNIT NUMBER

7. PERFORMING ORGANIZATION NAME(S) AND ADDRESS(ES)

Air Force Institute of Technology
Graduate School of Engineering and Management (AFIT/EN)
2950 Hobson Way
WPAFB OH 45433-7765

8. PERFORMING ORGANIZATION REPORT NUMBER

AFIT/ENP/GNE/05-04

9. SPONSORING/MONITORING AGENCY NAME(S) AND ADDRESS(ES)

Biomechanics and Modeling Branch
Human Effectiveness Directorate Det 5
Air Force Research Laboratories
Attn: Dr. Eric Holwitt DSN: 240-3583
Brooks City Base, Texas 78235 email: eric.holwitt@hedb.brooks.af.mil

10. SPONSOR/MONITOR'S ACRONYM(S)

11. SPONSOR/MONITOR'S REPORT NUMBER(S)

12. DISTRIBUTION/AVAILABILITY STATEMENT

APPROVED FOR PUBLIC RELEASE; DISTRIBUTION UNLIMITED

13. SUPPLEMENTARY NOTES

14. ABSTRACT

In this research, Bacillus anthracis spores were subjected to bursts of heat lasting on the order of one second in duration using a laser system to simulate the explosive environment from an agent defeat weapon. Heating times and temperatures were varied to establish a method to characterize the relationship between heating time, heating temperature, and spore viability. Two heating temperatures were examined at three variations of heating time ranging from 1.2 to 4.2 seconds. The higher temperature was adequate to neutralized the spore samples for both heating times. The lower temperature neutralized a portion of the spores during the shortest heating time, and sterilized the sample at the longest heating time. Before and after heating Raman spectra were obtained of the spores in order to characterize spectral differences related to neutralization by heat. Subtle spectral differences were identified with the 1013/cm peak resulting from CaDPA in the spore wall. This change indicates a change in the integrity of the spore wall resulting from the heating. Overall, a methodology was developed to correlate heating time, temperature, and spore lethality.

15. SUBJECT TERMS

Bacillus anthracis, Spores, Agent Defeat Weapons, Infrared Spectroscopy, Heat Inactivation

16. SECURITY CLASSIFICATION OF:			17. LIMITATION OF ABSTRACT	18. NUMBER OF PAGES	19a. NAME OF RESPONSIBLE PERSON
a. REPORT	b. ABSTRACT	c. THIS PAGE			Dr. Larry W. Burggraf (ENP)
U	U	U	UU	121	19b. TELEPHONE NUMBER *(Include area code)* (937) 255-6565, ext 4507

Reset

Standard Form 298 (Rev. 8/98)
Prescribed by ANSI Std. Z39.18